THE PETROCHEMISTRY OF THE ANKARA VOLCANICS, CENTRAL TURKEY

A thesis presented to the Faculty
of the State University of New York
at Albany
in partial fulfillment of the requirements
for the degree of
Master of Science

Department of Geological Sciences

Jay A. Ach

THE PETROCHEMISTRY OF THE ANKARA VOLCANICS, CENTRAL TURKEY

Abstract of

a thesis presented to the Faculty

of the State University of New York

at Albany

in partial fulfillment of the requirements

for the degree of

Master of Science

Department of Geological Sciences

Jay A. Ach

ABSTRACT

The Ankara volcanics comprise a small volcanic field immediately to the north of Ankara, Turkey. This volcanic field is composed of a mixture of flows, tuffs, and agglomerates, with the flows ranging in composition from high-K basaltic andesite to rhyolite. Dacitic flows are the most common. A potassium-argon date gives a Middle Eocene age of 42.0 $\pm$ 1.6 m.y. The volcanics unconformably overlie Paleozoic sediments of the "Cimmerian continent" to the south and Mesozoic rocks of the Ankara mélange to the north.

Results of analyses on 25 samples for major elements and Y, Sr, Rb, Ni, Cr, V, Co, Zn, Cu, Nb, and Zr are presented. Major elements and most trace elements show well defined trends when plotted on SiO_2 variation diagrams, indicating a chemical consanguinity. The processes of partial melting, fractional crystallization, and mixing/contamination are evaluated in terms of the roles they may have played in the generation of these magmas. A model based on fractional crystallization best explains the observed chemical trends; xenocrystic phases and disequilibrium phenomena in plagioclase indicate that mixing/contamination processes may have played a lesser role.

Comparison of major and trace element abundances of the Ankara rocks to those of other suites of calc-alkaline rocks reveals that these volcanic rocks most resemble those that have been produced by magmatic arcs built upon continental basement. This is consistent with the hypothesis that these rocks are related to the Eocene subduction and convergence which closed the northern branches of Neo-Tethys.

TABLE OF CONTENTS

Page

LIST OF FIGURES

Page

LIST OF TABLES

ACKNOWLEDGMENTS

I would like to express my utmost thanks to the director and many employees of the Maden Tetkik ve Arama Enstitüsü (M.T.A.) who made my field work in Turkey possible by providing me with logistical support, topographic maps, and accommodations in Ankara. Gultekin Savci deserves special thanks for guiding me through the bureaucratic mazes at the M.T.A., and also for the hospitality he and his family showed me. Erdal Herece spent several days in the field with me and provided valuable information on the geology of the Ankara region; I am most appreciative of his help. Celâl Abbas Özbek is possessed of great driving skills and proved to be a fine companion in the field.

A.M. Celâl Şengör, although unaffiliated with the M.T.A., still managed to be helpful on occasion. Assim Şengör and his family went out of their way to be hospitable and deserve many thanks.

A few folks in Albany also deserve mention. I am most grateful to John Bender for taking an interest in my work and spending so much of his time in discussions with me; his help was invaluable. Exposure to George Putman's petrographic prowess was both enjoyable and greatly appreciated. Julie Dyer proved to be as knowledgable as she is uncouth and made a great partner in crime. The unique personality of Pamela Stella proves that big things come in small packages; for your friendship, thanks Fish! The Dudes of the Earth provided much motivation to keep on keepin' on. Diana Paton did a superb job typing, expecially on the tables. I can never fully thank my parents for their unflagging support and encouragement, but I would like to say "thank you" anyway. Finally, thanks to the Chief, my mentor at Colgate, for providing me

with the "opportunity" to appreciate the beauties of petrology.

Funds for field and lab work were made available from NSF Grant #EAR 7904887 by S.E. DeLong.

INTRODUCTION

The geology of Turkey is both exciting and complex. Although generalized tectonic models of the country have been proposed (e.g. Şengör, 1981), the detailed geology of many areas remains to be explored, and the plate tectonic models evaluated in light of more complete data from the field and laboratory.

A study of the volcanic rocks in the Ankara region (Figure 1) was undertaken to determine their chemistry and to use those determinations to model their petrogenesis and to characterize the rocks as to a particular tectonic setting. This study began as a period of field work in the Fall of 1979 in which samples of the volcanic rocks in the small volcanic field to the north of Ankara (hereafter termed the Ankara volcanics) were collected. Subsequent laboratory investigations included observations of petrography and the determination of whole rock major and trace element geochemistry. These results are presented along with a petrogenetic model for the evolution of these rocks. Comparisons with other rock suites enabled a probable tectonic setting for their generation to be chosen.

Previous Work

The only previous study which has considered the Ankara volcanics in any detail was that of Gönül Büyükönal, who did a petrographic study of these rocks as her Ph.D. (1971). She concluded that this volcanic field was composed of various types of andesites.

E. Chaput mapped the Ankara area in two months in 1930 and published the resulting 1:135,000 map along with an explanatory text the

following year (Chaput, 1931). A new geological map of the Ankara area at the 1:500,000 scale was published by the Turkish Mining Exploration and Research Institute (M.T.A.) with accompanying text by Pamir and Erentoz in 1975. Other workers have investigated the areas around the Ankara volcanics, most notably Ozgul Erol, whose numerous papers are summarized, along with those of earlier investigators, by both Büyükönal (1971) and Pamir and Erentoz (1975).

CHAPTER I

GEOLOGICAL SETTING AND TECTONIC EVOLUTION

The Ankara volcanics are but one small portion of the widespread volcanism which has affected central Anatolia throughout much of its geological history. This volcanism has been produced by a complex series of collisional and convergent tectonic events. The principal events of the tectonic history of Turkey, with emphasis on central Anatolia, are briefly discussed below, as described principally by Şengör (1979), Şengör, Yilmaz, and Ketin (1980), and Şengör and Yilmaz (1981). The tectonic history of Turkey is discussed in detail in these papers and also by Ketin (1959, 1966), McKenzie (1972), Dewey, et al. (1973), Brinkmann (1976), and Dewey and Şengör (1979). Perusal of these papers is recommended for a more detailed account of the tectonics of this region than the brief summary which follows.

The pre-Permian tectonic history of Turkey is both complex and obscure and for this reason will not be discussed here. During the Permian, however, the area that is now Turkey formed part of the northern margin of Gondwanaland, facing Paleo-Tethys. This margin was an active one, involved in the southward subduction of Paleo-Tethys.

The principal event of the Triassic was the rifting away of the Anatolian region from Gondwanaland, forming the Cimmerian "continent", and opening up Neo-Tethys to the south. Also at this time, rifting of the Permian carbonate platform and subsequent early Jurassic convergence produced the short-lived Karakaya marginal sea.

The Jurassic saw the continued opening of Neo-Tethys at the expense of Paleo-Tethys, accompanied by fragmentation of the Cimmerian continent. This continental block broke up into a northern proto-Pontide volcanic arc (overlying the south-dipping subduction zone consuming Paleo-Tethys), the Sakarya "continent", the Anatolide/Tauride platform, and the Bitlis/Porturge massifs (Figure 2). This fragmentation also had the effect of producing a southern and northern branch of Neo-Tethys, with the latter also having the Izmir-Ankara Ocean as a branch. During the middle Jurassic, terminal closure of Paleo-Tethys occurred with the collision of the proto-Pontide magmatic arc with the Scythian platform of Laurasia. Continued convergence along this Pontide suture produced Tibetan-style volcanism in the late Jurassic.

From the mid- to late Cretaceous through the Paleocene, convergence dominated the tectonic picture. This manifested itself as the widespread emplacement of ophiolitic nappes throughout Anatolia and renewed subduction-related volcanism all along the Pontide arc, as a north-dipping subduction zone consumed the northern branch of Neo-Tethys. The Black Sea opened as a marginal basin behind this arc at this time. Subduction of the southern branch of Neo-Tethys was also occurring at various subduction zones further south during this time.

The early to mid-Eocene was characterized by continued arc volcanism in the Pontides with collisional events occurring along their length. These collisions took place diachronously, progressing from west to east. The Sakarya continent collided with the arc in the west, closing the Intra-Pontide Ocean, sometime between the Paleocene and the Lutetian. Slightly later, the Anatolide/Tauride platform also

Figure 2 - Paleogeographic map of the Anatolian region during the Early Jurassic (from Şengör and Yilmaz, 1981).

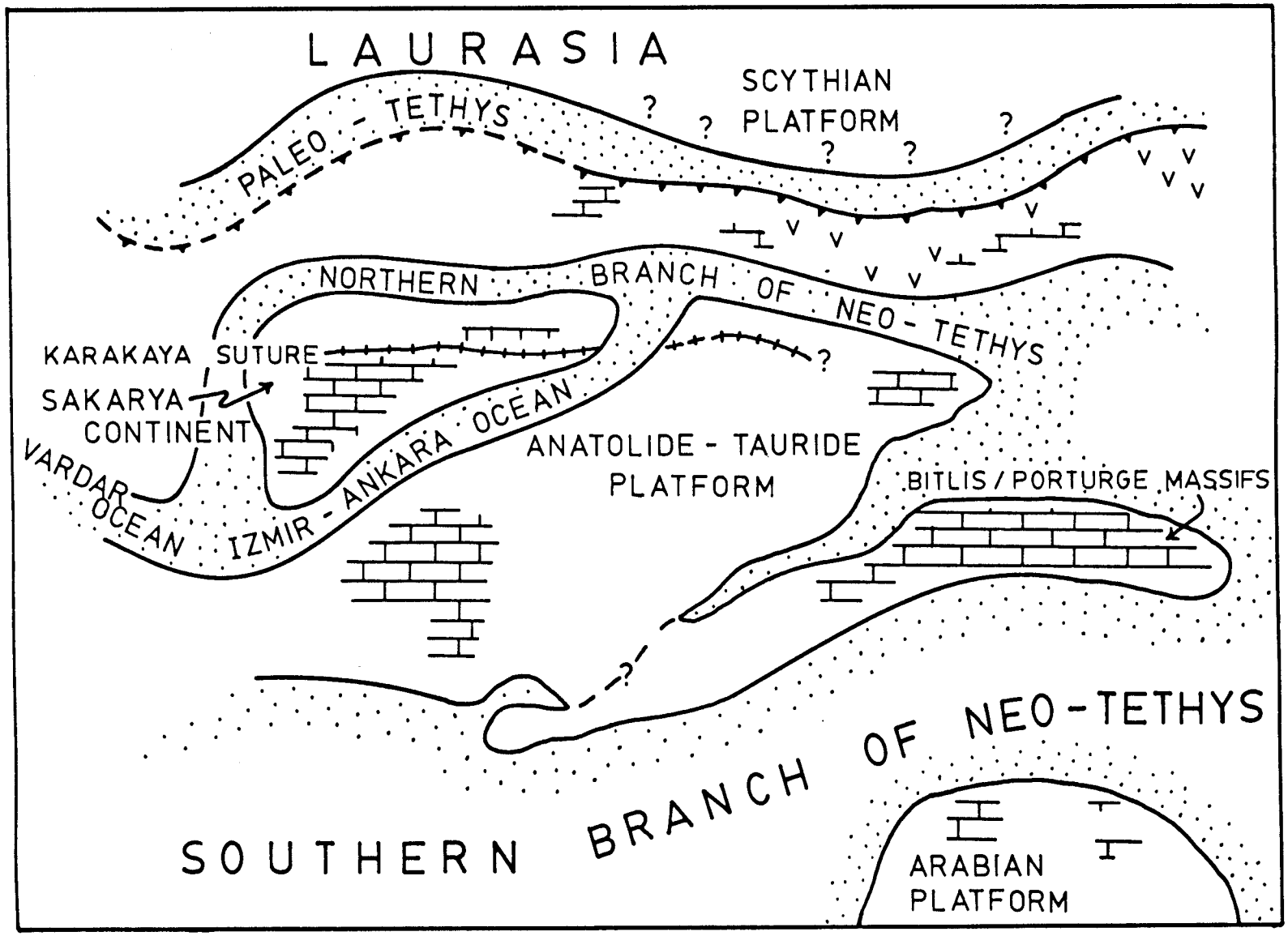
LAURASIA
SCYTHIAN
PLATFORM
PALEO - TETHYS
NORTHERN BRANCH OF NEO - TETHYS
KARAKAYA SUTURE
SAKARYA
CONTINENT
VARDAR
OCEAN
IZMIR - ANKARA OCEAN
ANATOLIDE - TAURIDE
PLATFORM
BITLIS / PORTURGE MASSIFS
SOUTHERN BRANCH OF NEO-TETHYS
ARABIAN
PLATFORM

collided, causing the internal imbrication of the platform which produced the south-verging Tauride nappe system, that buried the Anatolides. In the later portion of the Eocene continued convergence produced large amounts of crustal thickening and uplift, causing the extensive erosion which unroofed the Anatolide metamorphic massifs. This continued convergence also caused partial melting of the lower crust, as evidenced by calc-alkaline volcanism of this age, particularly in western Anatolia and the Aegean Islands. In southeastern Anatolia, the Eocene witnessed convergence between Anatolia and the Arabian platform, which closed several basins that made up part of the southern branch of Neo-Tethys.

Final closure of the southern Tethyan remnant, the Çunguş Basin, between Arabia and Eurasia, occurred in the early to middle Miocene. This collision deformed the East Anatolian Accretionary Complex and initiated the westward movement of Anatolia over the more easily subducted crust of the eastern Mediterranean. This displacement occurred along the North and East Anatolian Transform Faults.

The Pliocene to Recent has seen the continued operation of the neotectonic regimes set up in the Miocene. These can be divided into three tectonic provinces which, from east to west, are characterized as:

1) the East Anatolian compressional regime, located east of the Karliova triple junction and distinguished by north-south compression between Arabia and Eurasia, which has produced thickened crust (45 km?), thrust faulting, and Tibetian-style volcanism (Şengör and Kidd, 1979);

2) the Central Anatolia "Ova" regime, dominated by oblique strike-slip fault-bounded depressions (ovas) and mixed calc-alkaline and alkaline volcanism with extensive ignimbrites; and

3) the western Aegean extensional regime, characterized by large amounts (>30%) of crustal extension taken up by large east-west trending grabens with associated minor amounts of highly alkaline volcanism. The geology, geochemistry, and tectonics of this region have been addressed in detail by J.M. Dyer of this department in her master's thesis (1982).

Volcanism in Turkey has been widespread both spatially and temporally as would be expected from such a complex tectonic history. Subduction and collision related volcanism has occurred frequently, sometimes more than once in a given area due to different tectonic events. The Pontide region is a superb example of this, where an early magmatic arc over the north facing Paleo-Tethys subduction zone was the location of subsequent Tibetian-style volcanism following the collision of this arc with Laurasia. Later subduction of the northern branch of Neo-Tethys, with the Pontides as a south facing arc, followed by collision with the Anatolide/Tauride platform repeated the sequence of arc volcanism followed by collisional volcanism. Later dissection by the North Anatolian Transform and additional faulting and volcanism produced by the ova regime added further complexities to this region.

Subduction and collisional zones in Anatolia have generally progressed from north to south over time, and this is reflected in

the ages of the related volcanism. Additionally, Miocene to Recent volcanism shows progressive changes in chemistry from calc-alkaline in the east to Alkaline in the west due to the change in neotectonic regimes from strongly compressive to strongly extensional (Şengör and Dyer, 1979).

CHAPTER II

STRATIGRAPHY

The area around Ankara is characterized geomorphologically by a number of high hills and deeply incised stream valleys, providing abundant exposure of the rocks. The average elevation of the area is about 1,100 meters with the greatest elevations occurring in the southern portion in the hills surrounding Huseyingazi Tepe (el. 1,416 m). The rocks are generally flat-lying to moderately dipping. No folding was observed in the volcanics or the sediments within the volcanics. The tilting of these rocks is undoubtedly due to movements along the numerous faults observed cutting the volcanics and associated sediments.

Recent detailed mapping and careful study of the field relationships of the geology of the Ankara region have not been carried out, or if they have, remain unpublished and unknown to this author. The available recent literature on the area, i.e. Pamir and Erentoz (1975) and Büyükönal (1971), bases its stratigraphy on much older works dating primarily from before the turn of the century to the 1940's. As these older works are both obscure and predominantly written in Turkish, the stratigraphic information provided below is based primarily on the two recent sources, with additional information coming from Erdal Herece (personal communication) of the M.T.A. and from Chaput (1931).

As the focus of this study was the petrology and geochemistry of the volcanics in this area, little of the limited amount of available field time was spent studying the surrounding country rock.

Non-Volcanic Rocks

The basement of the Ankara region is composed of fragments of the former Cimmerian continent. Immediately adjacent to the field area, these stratigraphically lowest rocks are represented by mildly deformed greywackes, which crop out along the southern margin of the volcanics, where they are directly unconformably overlain by the volcanics. Slates(?), sandstones, and conglomerates, interbedded with limestones, are found just a few kilometers farther south in the Elma Dag (Elma Hill) area. Fossils found in these rocks date them as Permo-Carboniferous.

The Mesozoic is represented primarily by abundant fossiliferous Jurassic limestones with small quantities of clean, white quartzite. Chaput was able to subdivide the limestones into Liassic and "Later" Jurassic on the basis of faunal differences. These rocks are fairly widespread throughout the areas to the north, east, and west of the volcanics. Additionally, Chaput reports flysch containing limestone pebbles with minor serpentinites and other "roches vertes" associated with the limestone in some areas, such as northwest of Ankara. Other serpentinites were reported by Chaput from the Elma Dag area. Collectively, this assemblage of limestones, flysch, and serpentinites represents part of the 'Ankara Mélange' of Bailey and McCallien (1950) produced during the closure of the northern branches of Neo-Tethys.

Other than the volcanics, the Cenozoic is represented predominantly by Miocene(?) to Pliocene(?) fluvial to lacustrine sediments, consisting primarily of sands, clays, and marls. The basis for the assignment of these ages is unknown to this author. Büyükönal (1971) also notes a small, highly fossiliferous Eocene limestone outcrop, described by

an earlier author, just a few kilometers northwest of Ankara near Etlik, "associated with the agglomerates and tuffites". Additionally, at the northeast margin of the volcanics, a striking, coarse, brick red conglomerate is exposed. The clasts in this conglomerate are mostly metamorphics (Paleozoic(?) schists). This formation is assumed to be of lower Tertiary age, as red conglomerates frequently form the basal part of the Tertiary sequence. Quaternary alluvium fills most of the valleys.

Volcanic Rocks

The Ankara volcanics can be divided into three broad categories: tuffs, volcanic agglomerates, and flows, those three cropping out in approximately equal amounts. The tuffs are usually white and are eroded easily, thus usually appearing in the field as a very weathered, crumbly mass. Slightly less weathered outcrops sometimes exhibit weathered remnants of rock fragments; rounded quartz grains could sometimes be observed in hand sample. One exposure contains a number of rounded, dark colored, vesicular, glassy rock fragments up to a few centimeters in size, occurring in the lower portion of the outcrop. The tuffs were generally given only a cursory examination in the field due to the small likelihood of obtaining fresh samples for geochemical analysis.

The volcanic agglomerates covered a wide area and were spectacular in some outcrops. They consisted of rounded clasts of various other volcanic rocks (andesites and dacites)generally in a tuffaceous matrix. The clast size ranged from a few centimeters in diameter to sizes which dwarf the typical Anatolian. Generally, the clasts in

a given agglomerate are all of the same rock type, although these rock types vary from agglomerate to agglomerate. In certain instances, it is extremely difficult to distinguish an agglomerate from a flow because large clasts make up 80-90% or more of the outcrop, separated by only small amounts of matrix material. A pyroclastic (lahar ?) origin can easily be envisioned for the origin of the agglomerates.

The flows of the Ankara volcanics are predominantly dacitic or andesitic in composition with subordinate amounts of rhyolites and trachyandesites. Individual flows are difficult or impossible to distinguish in most cases, due to the deeply eroded nature of the terrain. Syn- and post-volcanic faulting has further obscured original relationships. Similarly, there is no obvious eruptive center, although Huseyingazi Tepe and its surrounding hills have been suggested as a possibility by Büyükönal.

The rocks are all highly porphyritic, with large plagioclase phenocrysts (up to 8 or 10 mm in length) predominating, and orthopyroxene, clinopyroxene, hornblende, and biotite also present in various combinations as phenocrysts. Quartz is also fairly frequently present, usually occurring as magmatically rounded and corroded grains. Fresh samples of the andesites range in color from grey to pink, depending upon the degree of oxidation which has occurred. Highly weathered andesites display a range of pastel colors including light grey, green, purple, and blue. Fresh samples of dacite were usually medium to dark grey in color, while the rhyolites were generally a light salmon pink.

Ages assigned to these volcanic rocks by Büyökönal and the previous investigators whom she reviewed range from "post Cretaceous" to

late Neogene. The one potassium-argon age done as part of this study gave a middle Eocene (Lutetian) age of 40.2± 1.6 m.y. (Appendix I). As this volcanic field is fairly small in size, it is assumed that volcanism here did not occur over a protracted length of time and that the entire suite is probably of similar age. The general geomorphological condition of the area when compared to the younger neotectonic volcanic terranes of east or west Turkey would tend to support the idea that Neogene to Recent volcanism has left this particular area unaffected.

In two localities, sedimentary deposits were noted to be intercalated with the volcanics. In one outcrop, just to the west of sample site 8-4, approximately 30 meters of fluvial conglomerates and sands, containing numerous, large, angular dacite clasts, were observed to overlie tuff and were in turn themselves overlain by the dacite flow of sample 8-4. In another area, located between Ankara and the Çubuk reservoir, a sequence of thin-bedded lacustrine sands and clays with mudcracks was observed within the volcanics. The exposed thickness of these sediments was about 25 meters.

CHAPTER III

PETROGRAPHY AND MINERALOGY

The Ankara volcanics exhibit a wide range of chemical compositions but are characterized by high alumina, relatively low magnesia, and moderate alkali contents. With the exception of the least silicic sample, the rocks are silica oversaturated and all are hypersthene normative (Table 1).

The whole-rock compositions of the 25 analyzed samples are plotted on a K_2O vs. SiO_2 chart, along with the classification scheme of Peccerillo and Taylor (1976), which was used to determine rock names in this study (Figure 3). Such chemical, rather than petrographic, classification schemes are now preferred for island arc volcanics and rocks of similar natures for reasons discussed by Peccerillo and Taylor. Most of the rock compositions fall in the dacite field, with a few in both the andesite and rhyolite field. One composition plots as a high-K basaltic andesite.

A few general petrographic observations hold true throughout the suite. The phenocryst population is dominated by plagioclase, and the assemblage plagioclase + hornblende + biotite + Fe/Ti oxides occurs in nearly all the samples. Frequent glomeroporphyritic clots of various combinations of these phases indicate coprecipitation. Quartz is also present in most samples,and the invariably rounded and embayed grain shapes indicate resorption by the melt. The ubiquity of the hydrous phases hornblende and biotite probably indicates crystallization under conditions of significant pH_2O.

TABLE 1: BULK CHEMISTRY AND NORMATIVE AND MODAL MINERALOGY OF THE ANKARA VOLCANICS

MAJOR ELEMENTS (Wt. %)

	2-4	11-9	7-4A	21-5	8-4	22-10	22-6	2-1	15-9	22-2	11-6B	7-2B	15-8	14-1B	11-6A	14-1A	21-2	1-2	15-3B	9-8B	9-9	9-12A	12-8	9-10	9-1
SiO_2	54.93	61.08	61.58	62.30	62.40	63.05	63.69	63.83	64.07	64.14	64.79	64.90	65.54	65.79	65.86	66.21	67.31	67.33	67.42	67.63	68.88	69.78	70.32	70.83	71.34
TiO_2	1.63	1.13	0.68	0.84	0.62	0.86	0.85	0.81	0.71	0.77	0.72	0.71	0.70	0.70	0.68	0.70	0.51	0.51	0.43	0.56	0.27	0.28	0.43	0.29	0.37
Al_2O_3	18.25	16.42	15.55	16.56	15.51	16.52	16.73	17.23	16.91	16.26	16.13	16.26	16.15	16.31	15.72	16.76	15.33	15.47	15.64	17.16	16.58	15.88	14.30	15.07	14.84
FeO*	6.67	5.12	4.99	4.40	4.40	4.29	3.99	4.21	4.03	4.09	4.02	4.09	3.69	3.60	3.73	4.02	3.07	3.06	2.99	3.23	2.09	2.66	3.00	2.19	2.29
MnO	0.12	0.06	0.04	0.05	0.08	0.02	0.08	0.07	0.05	0.07	0.03	0.04	0.00	0.03	0.07	0.01	0.03	0.05	0.05	0.00	0.02	0.01	0.01	0.04	0.01
MgO	2.73	2.06	4.04	2.55	4.11	2.39	1.94	1.10	2.59	2.12	1.14	1.23	1.22	1.34	1.86	0.51	1.92	1.92	2.02	0.54	0.57	0.40	0.57	0.71	0.50
CaO	6.81	5.68	5.89	5.33	5.82	5.31	4.81	4.51	5.11	4.13	4.58	4.64	4.24	4.33	4.36	3.68	4.02	4.07	3.92	4.11	3.04	3.17	3.27	2.86	2.31
Na_2O	4.55	3.83	3.52	3.50	3.50	3.91	3.79	4.11	3.63	3.88	4.05	3.98	3.99	4.12	3.90	3.91	3.71	3.74	3.99	3.71	4.12	4.29	3.55	4.31	3.89
K_2O	2.08	2.13	2.05	2.39	2.09	2.29	2.25	2.51	1.39	2.65	2.45	2.39	2.69	2.55	2.08	2.61	2.09	2.05	2.33	1.70	1.94	2.23	2.19	1.93	2.71
Cr_2O_3	0.01	0.00	0.05	0.00	0.01	0.00	0.00	0.00	0.00	0.00	0.00	0.00	0.00	0.00	0.00	0.00	0.00	0.00	0.00	0.00	0.00	0.00	0.00	0.00	0.00
Total	97.78	97.51	98.39	97.92	98.54	98.64	98.13	98.38	98.49	98.11	97.91	98.24	98.22	98.77	98.26	98.41	97.99	98.20	98.79	98.64	97.51	98.70	97.64	98.23	98.26
P_2O_5					0.21		0.29	0.18				0.24						0.23							
Na_2O+K_2O	6.63	5.96	5.59	5.89	5.59	6.20	6.04	6.62	5.02	6.53	6.50	6.37	6.68	6.67	5.98	6.52	5.80	5.79	6.32	5.41	6.06	6.52	5.74	6.24	6.60
100 MgO/M_2O+FeO (molar)	41.74	41.48	58.87	50.53	62.05	49.71	45.93	31.41	53.08	47.59	33.41	34.67	37.08	39.68	46.59	18.40	52.47	52.39	54.22	22.96	32.50	21.07	25.23	36.20	27.29

C I P W NORMATIVE MINERALOGY

q	--	13.40	12.78	15.35	13.98	14.85	17.47	16.30	19.94	16.81	18.38	18.68	19.18	18.93	20.94	21.99	24.25	24.10	22.00	27.65	28.56	26.88	31.24	29.54	31.00
c	--	--	--	--	--	--	--	--	0.14	--	--	--	--	--	--	0.81	--	--	--	1.74	2.18	0.65	0.14	0.69	1.31
or	12.29	12.59	12.11	14.12	12.35	13.53	13.30	14.83	8.21	15.66	14.48	14.12	15.90	15.07	12.29	15.42	12.35	12.11	13.77	10.05	11.46	13.18	12.94	11.41	16.02
ab	38.50	32.41	29.79	29.62	29.62	33.09	32.07	34.78	30.72	32.83	34.27	33.68	33.76	34.86	33.00	33.09	31.39	31.65	33.76	31.39	34.86	36.30	30.04	36.47	32.92
an	23.23	21.32	20.58	22.42	20.44	20.76	21.99	21.15	25.35	19.13	18.60	19.44	18.21	18.48	19.25	18.26	19.00	19.37	17.88	20.39	15.08	15.73	16.22	14.19	11.46
di	8.84	5.75	7.10	3.34	6.90	4.63	1.56	1.04	--	1.14	3.50	3.03	2.38	2.53	1.99	--	0.78	0.68	1.29	--	--	--	--	--	--
wo	4.41	2.86	3.61	1.68	3.52	2.33	0.78	0.51	--	0.57	1.72	1.49	1.18	1.25	1.00	--	0.39	0.34	0.65	--	--	--	--	--	--
en	1.82	1.16	1.93	0.80	1.98	1.10	0.34	0.16	--	0.26	0.56	0.50	0.42	0.48	0.44	--	0.19	0.17	0.32	--	--	--	--	--	--
fs	2.62	1.73	1.56	0.86	1.40	1.20	0.43	0.37	--	0.31	1.22	1.04	0.78	0.79	0.55	--	0.19	0.17	0.31	--	--	--	--	--	--
hy	10.84	9.89	14.68	11.48	14.06	10.15	10.13	8.73	12.77	11.08	7.31	7.94	7.45	7.58	9.50	7.51	9.25	9.31	9.27	6.35	4.85	5.44	6.24	5.39	4.86
en	4.44	3.97	8.13	5.55	8.25	4.85	4.49	2.58	6.45	5.02	2.28	2.57	2.62	2.86	4.19	1.27	4.59	4.62	4.71	1.34	1.42	1.00	1.42	1.17	1.25
fs	6.39	5.92	6.56	5.93	5.81	5.29	5.64	6.15	6.32	6.06	5.02	5.37	4.84	4.72	5.30	6.24	4.66	4.70	4.56	5.01	3.43	4.44	4.82	3.62	3.61
ol	0.97	--	--	--	--	--	--	--	--	--	--	--	--	--	--	--	--	--	--	--	--	--	--	--	--
fo	0.38	--	--	--	--	--	--	--	--	--	--	--	--	--	--	--	--	--	--	--	--	--	--	--	--
fa	0.60	--	--	--	--	--	--	--	--	--	--	--	--	--	--	--	--	--	--	--	--	--	--	--	--
il	3.10	2.15	1.29	1.60	1.18	1.63	1.61	1.54	1.35	1.46	1.37	1.35	1.33	1.33	1.29	1.33	0.97	0.97	0.82	1.06	0.51	0.53	0.82	0.55	0.70
Total	97.77	97.51	98.34	97.92	98.53	98.64	98.13	98.38	98.49	98.11	97.91	98.24	98.22	98.77	98.26	98.41	97.99	98.20	98.79	98.64	97.51	98.70	97.64	98.23	98.26

Estimated Volume Percent Phenocrysts — MODAL MINERALOGY

Plagioclase	10	15	4	55	5	20	45	35	30	30	20	10	30	25	25	15	20	30	30	3	15	20	25	10	15
Olivine	5	--	--	--	--	--	--	--	--	--	--	--	--	--	--	--	--	--	--	--	--	--	--	--	--
Orthopyroxene	--	2	5	2	10	5	2	]2	--	--	3	1	--	--	1	--	1	1	--	--	--	--	]1	--	--
Clinopyroxene	--	3	10	--	5	3	--		--	--	2	1	--	--	1	--	--	--	--	--	--	--		--	--
Hornblende	--	5	--	15	< 1	3	10	10	12	10	5	3	5	5	5	5	5	6	5	--	< 1	< 1	2	2	2
Biotite	--	5	1	1	< 1	2	1	2	5	5	5	3	2	2	2	2	3	2	2	3	5	5	3	3	5
Quartz	2	1	--	--	< 1	2	1	< 1	2	3	< 1	< 1	1	2	< 1	1	--	--	1	3	5	3	2	15	7
Fe-Ti Oxides	1	1	1	2	1	1	2	1	1	2	1	1	2	1	1	2	1	1	2	1	1	1	1	1	1
TOTAL	18	32	21	75	24	36	61	51	50	50	37	20	40	35	36	30	30	40	40	10	30	30	34	31	30

Figure 3 - K_2O vs. SiO_2 classification of the calc-alkaline rocks (from Peccerillo and Taylor, 1976). Compositions of the Ankara volcanics are plotted as open circles.

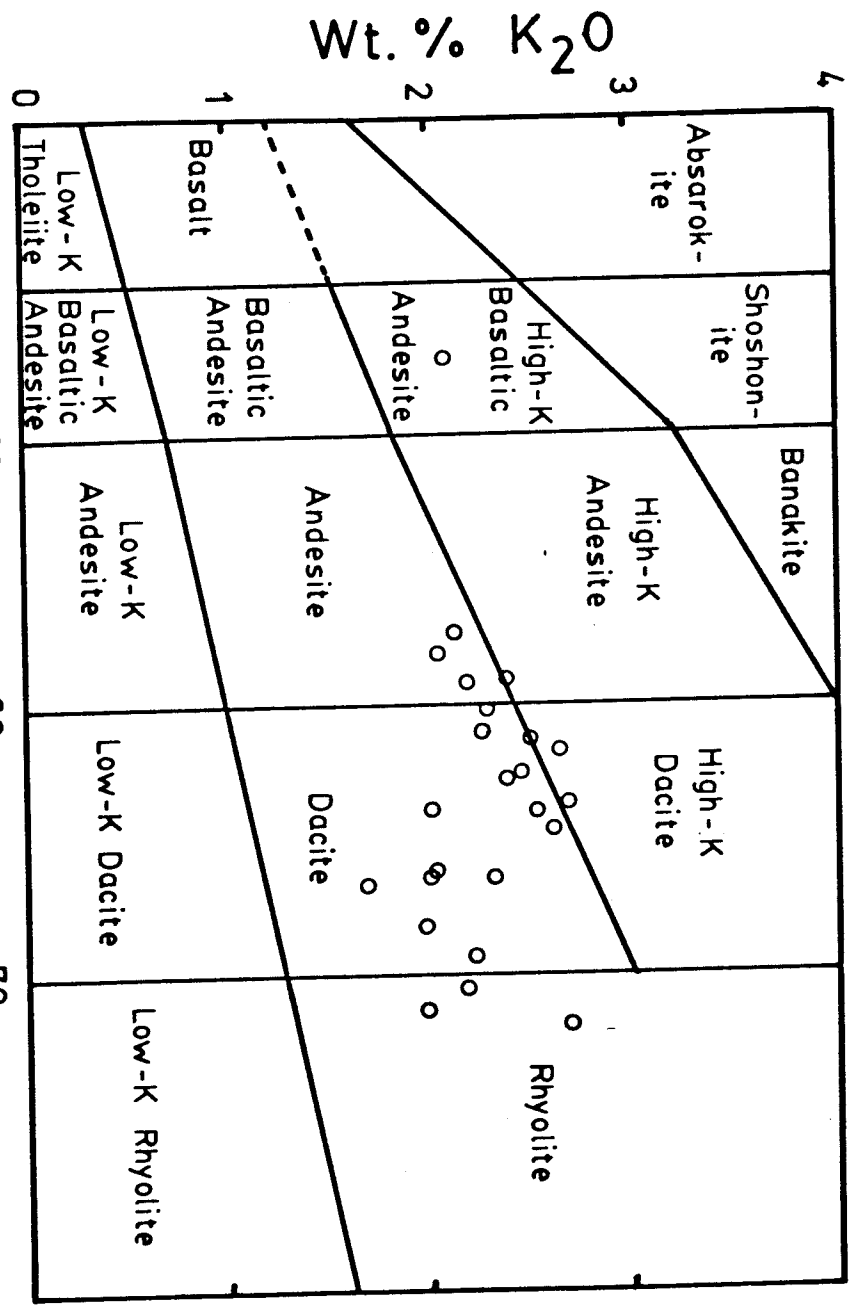
Wt. % K_2O
4
3
2
1
0
Absarok-ite
Shoshon-ite
Banakite
High-K Basaltic
Andesite
High-K Andesite
High-K Dacite
Basaltic Andesite
Andesite
Dacite
Rhyolite
Basalt
Low-K Basaltic Andesite
Low-K Andesite
Low-K Dacite
Low-K Rhyolite
Low-K Tholeiite
52
56
63
70
Wt. % SiO_2

In the following sections, a generalized petrographic description of each of the rock types is presented. Descriptions of individual samples can be found in Appendix II. Approximate phenocryst modal abundances are listed in Table 1. Microprobe mineral analyses are listed in Appendix III and comments on mineral chemistry are included in the following descriptions.

High-K Basaltic Andesite

The one sample of high-K basaltic andesite is black and fine-grained with noticeable plagioclase phenocrysts. The plagioclase grains are slightly rounded to euhedral and range up to 4mm long. Most grains exhibit oscillatory zoning, although some are simply continuously zoned. The grains usually occur singly, although sometimes in pairs or small clots. Slight antiperthite textures were observed in some grains.

Olivine occurs as anhedral to euhedral grains up to 1mm across. The larger grains have rims of iddingsite, with the smaller ones being completely replaced by this mineral. Slight zoning was observed in some grains. The composition was determined optically to be around Fo_{75}.

Quartz is also present in this rock, in large grains (up to 3mm in diameter) that display magmatically rounded and corroded shapes. Microcrystalline rims of clinopyroxene around the quartz also indicate reaction with the melt.

Other phases present include numerous grains of an anhedral opaque phase and a few pseudomorphs of pyroxene after hornblende. The groundmass is composed dominantly of plagioclase laths with some glass and a few clinopyroxene microphenocrysts.

The occurrence of both magnesian olivine and quartz in this rock indicates a disequilibrium condition. Norm calculations (Table 1) indicate a silica undersaturated composition and these together with textural relationships lead to the conclusion that the quartz is xenocrystic in nature. The plagioclase with antiperthite lamellae and the hornblende (pre-pseudomorphed) are also probably xenocrystic.

Andesites

Four rocks are classified as andesites. They are dark grey to black in hand sample and are porphyritic and fine-grained to glassy in texture, sometimes also vesicular. These rocks are characterized by high proportions of orthopyroxene and clinopyroxene phenocrysts and clots with plagioclase as the other major phenocryst phase. A moderate to strong flow fabric is evident in the groundmass.

The size of plagioclase phenocrysts is quite variable, with the largest grains about 8 mm long. They are euhedral or slightly rounded in shape, with a few broken grains present; some euhedral grains exhibit rounded (more sodic?) cores. Oscillatory, patchy, continuously, and discontinuously zoned phenocrysts can all be observed, along with zones of dendritic or skeletal growth. Inclusions of fluid and rod-shaped crystallites are both common. The two available microprobe analyses of two points in separate grains give compositions of AN_{46} and AN_{52}. Lack of good twinning and the complexity of the zoning discouraged optical determination of plagioclase compositions in the entire suite of rocks studied.

Orthopyroxene occurs in the andesites as euhedral phenocrysts up to 2mm long which are found either singly or in clots with or without

clinopyroxene. Zoning is often evident in the orthopyroxenes, the zoned grains having pleochroic cores and non-pleochroic rims. Other grains are unzoned and exhibit varying degrees of pleochoism. Occasionally, a grain will contain a few exsolution lamellae of clinopyroxene. Eight microprobe analyses (Appendix III) give a compositional range of enstatite to bronzite, EN86-77 WO3-4 FS11-19.

Clinopyroxene in the andesites is similar to orthopyroxene in size, shape, and habit, and is frequently twinned. Slight zoning can be observed under crossed Nichols in some grains. Probe analyses (EN61-43 WO45-25 FS9-11) classify the clinopyroxene as endiopside.

The highly magnesian character of both the ortho- and clinopyroxene is an obvious feature of these minerals. Their overall chemistry is similar to that of pyroxenes from much more basic rocks, e.g. Tables 3 & 16 in Deer, Howie, and Zussman (1978). Such compositions can also be derived under conditions of high pO_2 (Ashwal, et al., 1979), but their high Cr_2O_3 contents (up to 0.72% in orthopyroxene, 0.59% in Cpx), their high alumina contents, and their occurrence in mono- or biminerallic clots suggests that they are xenocrysts/xenoliths of a pyroxene cumulate of possible mantle derivation.

Biotite is present throughout the andesites either as single grains up to 2-3 mm across, or associated with some combination of hornblende, plagioclase, and opaques in glomeroporphyritic clots. It is brick red-brown and strongly pleochroic in plane light. The single grains are usually rounded to somewhat embayed; those in clots have irregular outlines defined by the other grains in an interstitial relationship. Resorption of biotite by the melt is indicated by the rounded and embayed shapes; other grains indicate

a reaction relationship, as they are rimmed by anhydrous phases, predominantly plagioclase and opaques. Pseudomorphs of finely divided opaques after biotite indicate decomposition of the phase upon the rapid pressure decrease and loss of volatiles associated with extrusion.

Also present throughout the andesites is hornblende, which occurs in a wide range of sizes, reaching 8mm in length in some samples. Two varieties (rarely in the same rock) can be observed under plane light, one lime green and the other golden brown; both are pleochroic. Numerous inclusions of apatite, plagioclase, and opaques are present, particularly in the green variety. Hornblende in the andesites is frequently altered in the same two ways as biotite; either magmatically to anhydrous phases (dominantly orthopyroxene) or by eruptive pressure/volatile changes to pseudomorphs composed of fine, dusty opaques.

Quartz occurs sparingly as fairly small (to 1 or 2mm) rounded to embayed grains. The quartz in two samples, 7-4 and 8-4, is surrounded by microcrystalline rims of clinopyroxene. Simple resorption of grains may be explained as a pressure-temperature change phenomenoma occurring as the magma rises or erupts. The reaction relationship indicated by the clinopyroxene rims argues for a xenocrystic origin, however, for the quartz in at least the two samples where this phenomenom is observed. Additional evidence for a quartz + melt → clinopyroxene reaction can be found in sample 11-9 and again in sample 8-4. In these rocks circular groups of inwardly radiating clinopyroxene needles were observed. These appear identical to a clot pictured by Eichelberger (1978, Figure 2d) and interpreted by him to represent

such a reaction carried to completion.

The mesostasis of the andesites is composed of a large proportion of glass containing rod-shaped crystallites, with microlites and microphenocrysts of plagioclase and minor amounts of pyroxene, hornblende, and opaques.

Dacites

Dacites form the largest compositional group within the suite of rocks studied, numbering seventeen. They are generally compact and range from medium grey to pink in hand sample. Large plagioclase crystals dominate the phenocryst population, but in addition to the feldspar, large hornblende, quartz, and/or biotite are often visible in hand specimen. In thin section, it becomes evident that the assemblage plagioclase + hornblende + biotite + quartz + opaques is present throughout most of the dacites. Orthopyroxene and clinopyroxene are usually only present as relatively minor phenocryst phases and are absent from the most silicic members of this group.

The textures of the dacites, besides being porphyritic, are hyalopilitic to pilotaxitic,with some degree of flow fabric usually present in the groundmass. Phenocrysts sometimes appear to be crudely aligned, but in other cases their orientation appears totally random. Numerous broken grains are often present in these latter rocks.

Plagioclase in the dacites has a very large size range, from microphenocrysts to grains greater than 1 cm long. Most grains are euhedral, although some are sharply broken. Others are rounded, and partially resorbed margins were noted on a few grains. As in the andesites, some euhedral grains have rounded (more sodic?)cores.

The plagioclase occurs as either single crystals or in glomeroporphyritic clumps, alone or with other minerals. Clumps with very large grains tend to be monominerallic. Oscillatory zoning is both very common and very strong when present; grains with oscillatory zoning also frequently exhibit areas of patchy zoning, commonly in the cores. Continuous, discontinuous, and reverse zoning are also observed in various grains. Additionally, zones of dendritic and skeletal growth are not uncommon. Such zones have been interpreted by several authors (e.g. Hibbard, 1981; Lofgren, 1974) as representing periods of rapid crystal growth under supercooled conditions. Inclusions of fluid, crystallites, and occasionally small hornblendes are frequent. Microprobe analyses fall in the range AN_{34-58}.

Hornblende is common throughout the dacites, usually as euhedral crystals, but some grains are slightly rounded or embayed. Grains range up to 8mm long. Most hornblende is green, but brown hornblende is present in a few samples; both varieties usually occur as individual grains, but the inclusion of hornblende in glomeroporphyritic clots with plagioclase, biotite, and opaques is not uncommon. Inclusions within the hornblende are frequent and consist primarily of small plagioclase grains, apatite, and zircon. The embayed and rounded shapes indicate resorption by the melt when these shapes are present. In other samples, rims of small orthopyroxene grains and total replacement by orthopyroxene indicate a dehydration reaction has occurred. In still other rocks, hornblende is represented only as pseudomorphs composed of dusty opaques, as in some of the andesites. These pseudomorphs again are interpreted to be products of rapid eruptive P-T changes. Compositions of three green hornblendes are given in Appendix III.

Biotite is present usually as rounded or embayed forms, but is sometimes euhedral. Grains in some rocks are up to 3mm in diameter, and inclusions of apatite, zircon, and opaques are fairly frequent. In some dacite samples, the biotite has decomposed upon extrusion to pseudomorphs composed of very fine-grained opaques.

Orthopyroxene occurs as small to medium euhedral grains (up to 2mm) and is usually pleochroic, indicative of a hypersthene composition. As in the andesites, it occurs mostly as single grains or less frequently in small clots by itself or with clinopyroxene. Lesser amounts of orthopyroxene are found as reaction rims on hornblende or as replacements (pseudomorphs) of this mineral. In sample 1-2, a large, corroded hypersthene grain with a rim of small hornblende grains was observed, indicating the reverse orthopyroxene → hornblende reaction. Additionally, sample 15-3B contains orthopyroxene mantled by a thin clinopyroxene or pigeonite rim, suggesting a possible xenocrystic origin for those particular grains. Small amounts of microphenocrystic orthopyroxene are found in some samples.

Clinopyroxene is much less common than orthopyroxene in the dacites. When it occurs, it exhibits similar size, shape, and habit to the orthopyroxene described above, except that it is restricted to the phenocryst population with only two exceptions. Optical similarity to the analyzed clinopyroxenes in the andesites indicates a probable endiopside to augite composition. However, in sample 15-3B, one xenocrystic grain of (titano-?) aegirine-augite was observed.

Quartz is found in nearly all the dacites in various quantities and sizes, from a few scattered small grains to fairly numerous, large (up to ~ 6 mm) grains. Rounded or embayed grain shapes are the rule;

however, one euhedral grain with slight embayments was observed, suggesting at least some of the quartz precipitated from the melt, then was later resorbed upon a change in P-T conditions or bulk composition.

Minor phases present include opaques, zircon, and apatite. Small grains (<0.5mm) of opaques are numerous throughout, with a few larger grains (up to 1 mm) present. They exhibit anhedral to euhedral shapes, with the high frequency of isometric shapes indicating that magnetite (Ti-rich?) probably predominates. Zircons are present as anhedral to euhedral inclusions in hornblende or biotite, or as isolated grains in the groundmass. These latter grains can be surprisingly large with some up to 0.2 mm long. Apatite is also fairly widely distributed, usually occcurring as anhedral inclusions in hornblende and, to a lesser extent, in biotite.

In several of the samples of both andesites and dacites, xenoliths of fine-grained, densely intergrown plagioclase laths and hornblende can be found. Such xenoliths may easily be observed in outcrop at site 2-1, where they occur as rounded, golf ball to softball-sized maroon masses within the lighter pink dacite. These may represent pieces of a chilled margin, although xenoliths with identical textures have been interpreted by Eichelberger (1978) to represent blebs of mafic magma chilled when mixed with a cooler, more felsic magma.

The groundmass of the dacites is composed primarily of glass, sometimes partly devitrified, with numerous minute, rod-shaped crystallites. Microphenocrysts appear in the groundmass in varying

quantities. Most are plagioclase, with lesser orthopyroxene, clinopyroxene, or hornblende appearing on occasion.

Rhyolites

The three rocks classified as rhyolites are characterized by porphyritic and hyalopilitic to pilotaxitic textures. The large quartz phenocrysts are especially distinctive in hand specimen. The phenocryst assemblage consists of plagioclase, biotite, quartz, and hornblende.

Plagioclase occurs as medium to large (up to 6mm) euhedral, rounded, or sharply broken grains. All grains are zoned, with strong oscillatory zoning most common, although continuously and discontinuously zoned grains can also be found.

Biotite is present as large (up to 3mm) euhedral to rounded plates. In plane light, sections perpendicular to the c-axis are strongly pleochroic from light yellow-green to bright orange-red; basal sections are brick red. Some grains have irregular corroded edges and rims of opaques and plagioclase, indicating a dehydration reaction. A few relict grains composed of fine opaques can be observed in one sample. Inclusions of apatite and small plagioclase are not infrequent.

Quartz is a very common phenocryst phase in the rhyolites, occurring in these rocks in both greater abundance and size than in the andesites or dacites. The rounded to embayed grains can reach sizes of about 8 mm in diameter.

Conversely, hornblende is not quite as common in the rhyolites as in the previously discussed rock groups. It occurs in small euhedral

phenocrysts (up to 3mm) and is red-brown in cross section. Other sections exhibit very strong yellow-green to red-brown pleochroism. Relict hornblende grains composed of finely divided opaques are sometimes present. As with the other rock types, such relict grains of both hornblende and biotite were probably produced by decomposition of these phases upon extrusion.

Minor phases are the same as in the dacites, including opaques, zircons, and apatite. Shape again suggests that the abundant, small, euhedral to anhedral opaque grains are (titano?) magnetite.

In summary, the petrography of the Ankara volcanics reveals some generally consistent overall trends including: the dominance of the plagioclase + hornblende + biotite + opaques assemblage; the occurrence of pyroxene predominantly in the less silicic samples; and the increase of biotite relative to hornblende in the most silicic. Many complexities are also revealed, including disequilibrium phase assemblages, anomalous phase chemistries, reaction and resorption of various phases by the melt, and complex zoning. Combined, these observations indicate that while it may be possible to explain this suite of rocks as the products of a single simple petrogenetic process, the actual history must be more complex. At the least, this history probably involves the addition of one or more xenocrystic phases, and the possibility of other disequilibrium processes or more complex multiple source crystal/liquid interactions cannot be ruled out by petrography alone.

CHAPTER IV

GEOCHEMISTRY

Geochemical Data

Major element data (nine elements) are presented below for 25 samples of volcanic rocks from the study area along with trace element analyses. Abundances were determined for the following trace elements: zirconium, niobium, yttrium, strontium, rubidium, zinc, copper, nickel, chrome, vanadium, and cobalt. A potassium-argon age determination for one sample is presented in Appendix I.

Analytical Methods

Eighty-seven samples of volcanic rocks were collected from the field area. To determine which samples to analyze chemically, a thin section of each sample was made and examined. Selection of the sample suite to be analyzed was then made with the following criteria in mind:

1) the suite of samples to be analyzed should be as fresh and unaltered as possible;
2) the sample suite should represent the entire range of volcanic rock compositions present in the area; and
3) rocks of obvious pyroclastic origin should be excluded, because such rocks may have been considerably affected by selective sorting (e.g. Walter, 1972).

Twenty-five samples meeting these criteria were selected for chemical analysis.

Hand samples from the field were broken into several pieces with a hydraulic rock splitter and approximately 200 grams of each sample was selected for analysis. To reduce the large pieces to <100 mesh powder, they were first broken into pieces 2 cm in size with a hammer on a hardened steel plate. Obviously altered or weathered fragments were discarded. This material was then crushed further in a cylindrical hardened tool steel mortar and pestle to sand-sized grains. The final stage involved careful grinding by hand in a high purity alumina ceramic mortar and pestle until the entire sample passed a 100 mesh nylon sieve. All implements employed were meticulously cleaned after each sample to avoid cross-contamination.

Analysis for major elements was done on unfluxed fused glass beads made on a molybedenum strip furnace, where they were fused rapidly (~ 30 sec.) under ~3 atm argon pressure to minimize alkali loss. To insure sample homogeneity, the glasses were ground in an agate mortar and pestle after their first fusion and were refused under the same conditions. The glass beads produced were mounted with epoxy in phenolic discs, ground, polished, and analyzed by microprobe.

Actual analysis of the beads was carried out on the four spectrometer ARL-EMX-SM electron microprobe located at the State University of New York at Stonybrook, using a number of mineral and rock standards. An accelerating voltage of 15kv and sample current of 0.015 microamps were used. The data were reduced using the methods of Bence and Albee (1968) and matrix corrections modified by Albee and Ray (1970). A diffuse spot of approximately 150 micron size was used for all analyses on glass beads. A smaller spot was used for mineral analyses. A few additional mineral analyses were performed on the Harvard ARL microprobe, under similar operating conditions.

The trace element analyses were done by x-ray fluorescence on pressed powder pellets. These pellets were backed with boric acid and were pressed under vacuum. The analyses were done at Woods Hole Oceanographic Institute on the Philips USA - AXS automated XRF spectronomer located there, using pressed powder samples of U.S.G.S. reference rocks as standards.

Microprobe precision and accuracy is generally 2-5% of the amount present, with SiO_2 usually less than 1%. Precision and accuracy for trace elements run on the Woods Hole XRF is usually between 1 and 5% (Schroeder et al., 1980). However, less than optimum run conditions produced less accurate values for these samples. Accuracy is approximately as follows: 5% for Sr, Cu, Cr, and Co; 10% for Zn; 15% for Y and Nb; 20% for Rb, Zr, and V; and 25% for Ni. An analysis of the standard BR and the accepted WHOI values for that standard are included in Table 3 for comparison.

Major Elements

The results of major element analyses of 25 samples of the Ankara volcanics are presented in Table 1, along with their corresponding calculated CIPW normative mineralogy and their estimated modal mineralogy.

To facilitate recognizing overall trends and intersample relationships, the major element data are presented in Figures 4 and 5 as binary oxide plots with silica as the abcissa. It is readily apparent that the abundances of most elements decrease with increasing silica content. The exceptions are Na_2O, which progressively increases, and K_2O, which first increases, then after about 66% SiO_2, begins to decrease.

These rocks are all hypersthene and (except for the low silica

Figure 4 - Major elements: Al_2O_3, TiO_2, FeO*, and MnO vs. SiO_2.

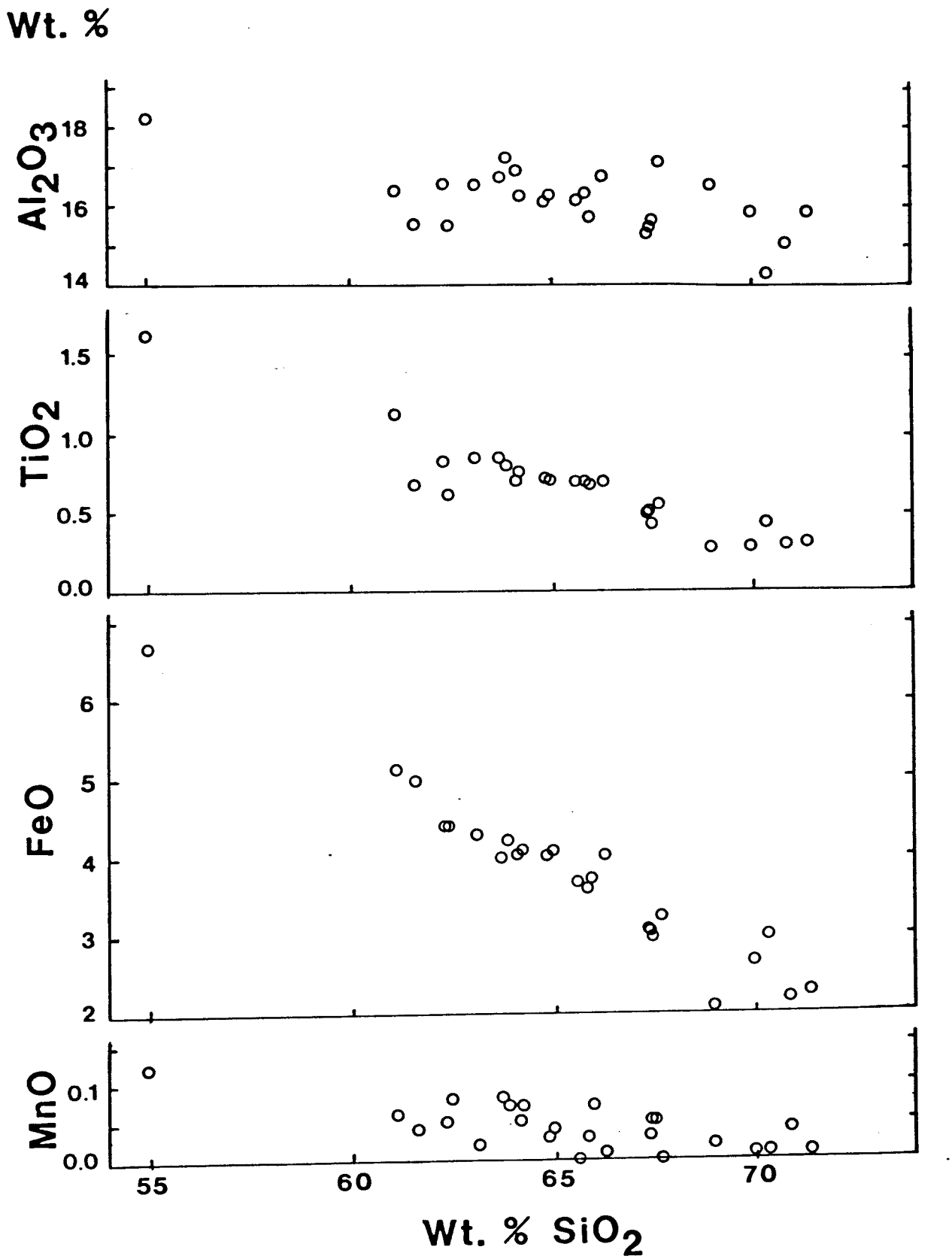
Wt. %
Al2O3
18
16
14
TiO2
1.5
1.0
0.5
0.0
FeO
6
5
4
3
2
MnO
0.1
0.0
55
60
65
70
Wt. % SiO2

Figure 5 - Major elements: MgO, CaO, Na_2O, and K_2O vs. SiO_2.

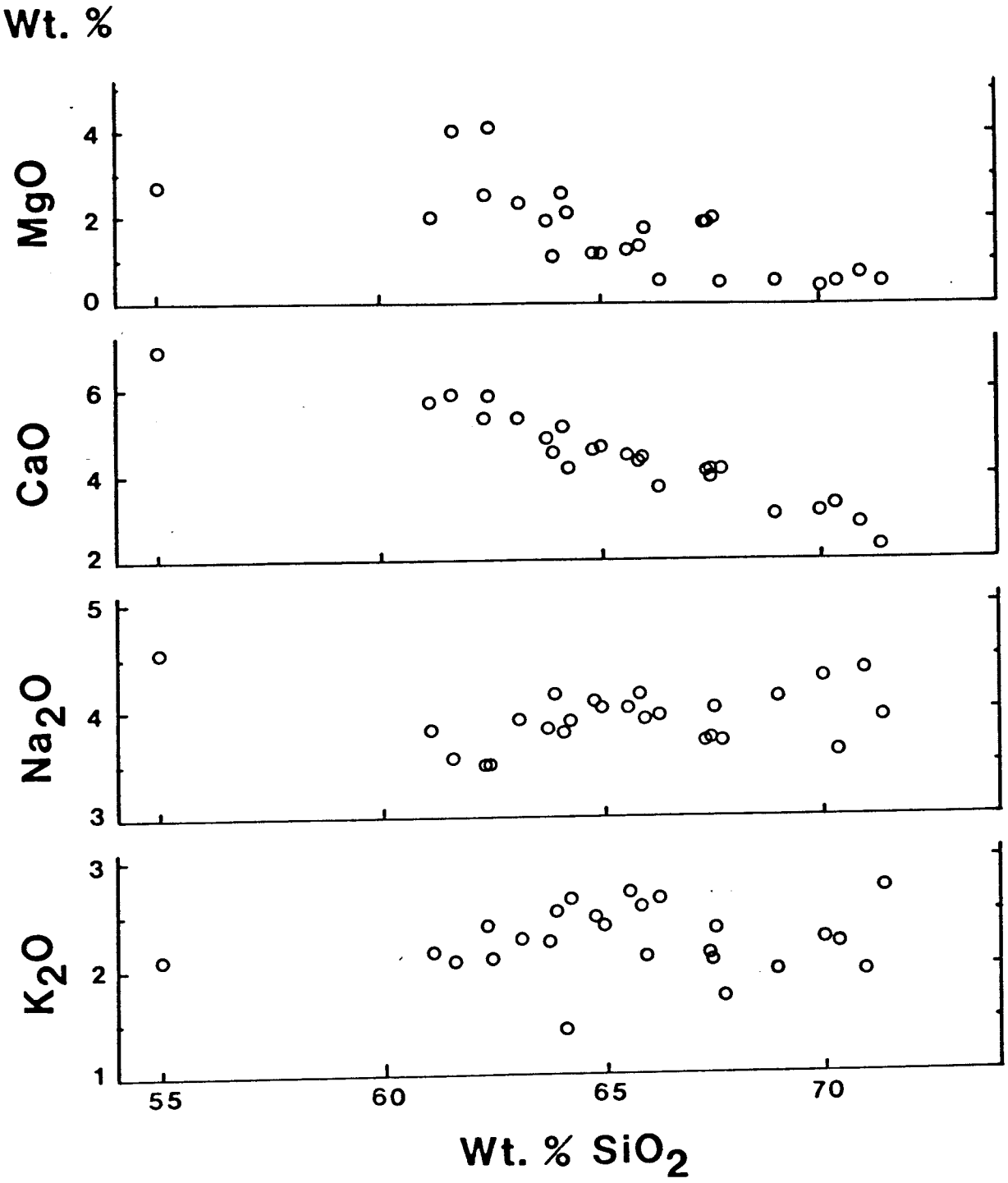
Wt. %
MgO
4
2
0
CaO
6
4
2
Na_2O
5
4
3
K_2O
3
2
1
55
60
65
70
Wt. % SiO_2

sample) quartz normative. When their composites are plotted in terms of Na_2O + K_2O, FeO*, and MgO (AFM), the resulting trend, showing little iron enrichment, is indicative of the calc-alkaline series (Figure 6).

The major elements show similarities to volcanic rocks from active plate margins, including high Al_2O_3 contents, low MgO and TiO_2 contents, and generally low molecular MgO/FeO* + MgO (e.g. Whitford, et al., 1979). The rocks classified as dacites are quite similar to dacites from island arcs/Andean margins with continental basement, e.g. the Taupo Volcanic Zone, New Zealand, and the Cascade Range of the U.S. (Table 2). These close similarities strongly suggest that these rocks are products of a similar tectonic setting.

In summary, the major element data show good internal correlation throughout the Ankara volcanics. These data also demonstrate the close chemical similarity of these lavas to those from active plate margins, particularly those with volcanic arcs built upon continental crust.

Trace Elements

The results of analyses for 11 trace elements (Zr, Y, Sr, Rb, Zn, Cu, Ni, Co, Cr, V, Nb) are presented in Table 3.

Variation diagrams with each of these elements plotted against silica are presented in Figures 7, 8, and 9. The immediately striking feature of these diagrams is that they indicate that apparently none of the normally incompatible elements (Rb, Zr, Nb, Y) exhibit incompatible behavior in this rock series (Figure 7). Rubidium roughly parallels potash in behavior, increasing (as is usually expected) with increasing silica until about 66% SiO_2, then generally decreasing. The high field strength ions Zr and Nb show an erratic behavior with

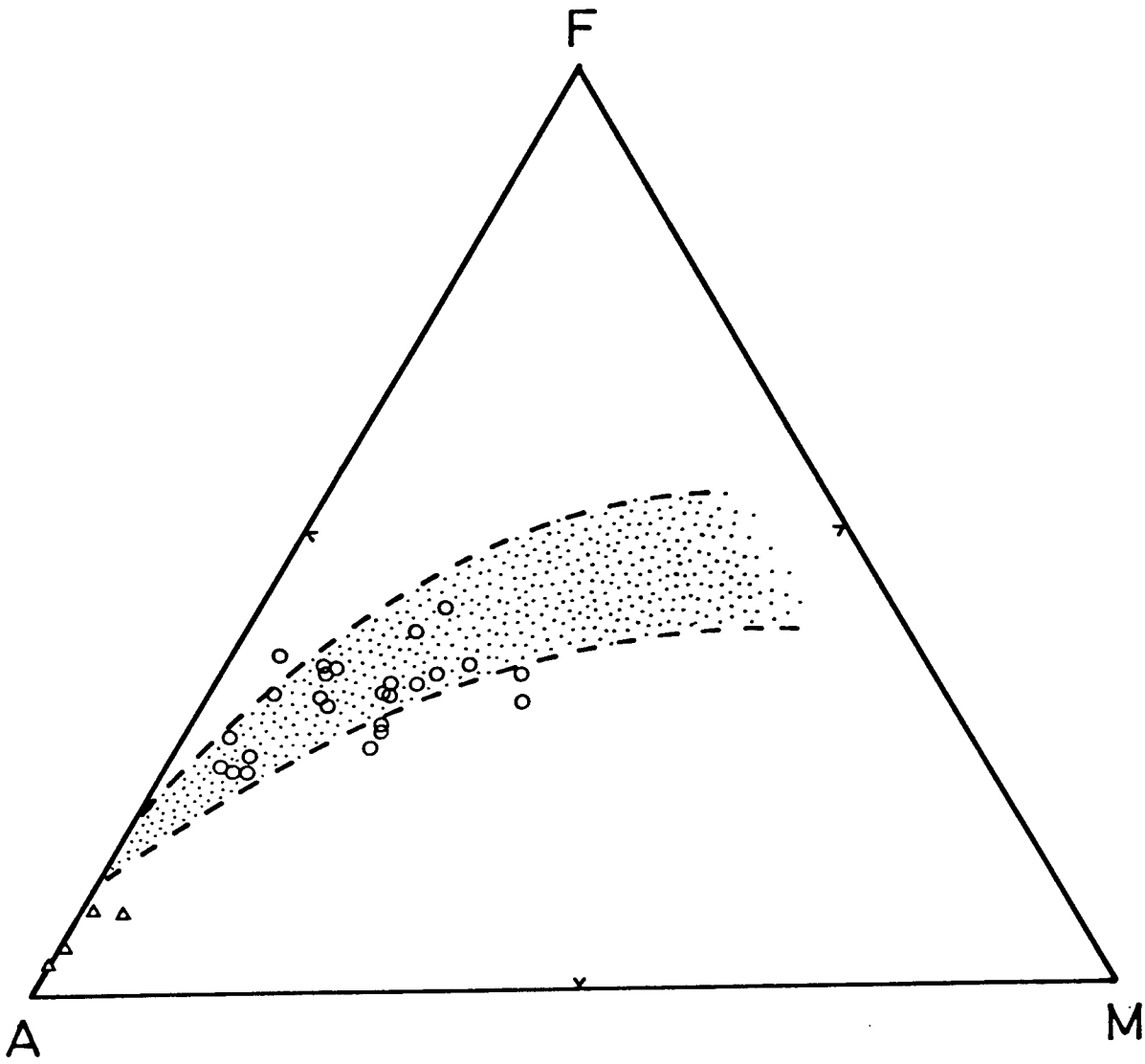

Figure 6 - AFM (Na_2O + K_2O, FeO*, MgO) diagram showing compositions of the Ankara volcanics. Open circles represent whole-rock compositions and triangles represent compositions of glass in thin sections. The calc-alkaline trend of Ringwood (1977) is indicated by the stippled area. His trend is based on the trends displayed by rocks from the Cascade, Aleutian, and New Zealand calc-alkaline provinces.

TABLE 2: COMPARISON OF THE AVERAGE DACITE COMPOSITION OF THE ANKARA VOLCANICS TO THOSE OF SOME OTHER AREAS. NUMBER IN PARENTHESES INDICATES NUMBER OF SAMPLES INCLUDED IN AVERAGE.

	Ankara volcanics average dacite(17)	Mt. Lassen Southern Cascades average dacite(4)*	Medicine Lake Highlands Southern Cascades average dacite(6)*	Taupo Volcanic Zone New Zealand average dacite(8)*
SiO_2	65.90	66.1	67.2	66.2
TiO_2	0.63	0.4	0.4	0.4
Al_2O_3	16.30	16.4	16.2	15.3
FeO	3.58	3.5	3.6	3.9
MnO	0.04	0.07	--	0.1
MgO	2.05	2.1	1.4	2.2
CaO	4.24	4.4	3.5	4.4
Na_2O	3.93	3.9	3.9	3.5
K_2O	2.24	2.2	3.3	2.3

* These averages are from Eichelberger (1975), who compiled the analyses from various other sources.

Table 3 - Trace element concentrations (ppm) of the Ankara Volcanics

Element	2-4	11-9	7-4A	21-5	8-4	22-10	22-6	2-1	15-9	22-2	11-6B	7-2B	15-8	14-1B
Y	28.8	24.6	25.2	20.0	22.2	20.2	24.6	21.8	22.1	23.6	27.9	25.4	22.2	21.5
Sr	632.0	408.7	427.9	482.6	446.4	501.3	492.6	493.5	416.5	354.8	385.9	425.1	388.0	395.6
Rb	46.2	70.0	66.4	63.1	72.9	64.5	74.8	73.5	196.3	70.4	76.8	74.6	75.0	71.3
Ni	23.1	31.2	169.5	18.3	109.2	61.8	16.4	21.9	18.7	11.9	20.3	20.7	17.0	19.3
Cr	15.3	46.1	304.3	24.6	159.3	99.1	7.7	25.0	15.2	11.4	21.1	20.0	21.7	17.2
V	165.9	121.8	72.3	100.5	110.9	115.6	92.9	81.6	88.7	82.2	86.6	85.2	94.7	99.3
Co	22.7	15.5	21.0	12.4	19.8	15.3	11.2	11.0	12.5	10.3	10.3	11.5	10.4	9.7
Zn	63.9	46.7	53.8	62.4	50.2	55.7	45.6	55.3	43.8	42.2	47.6	48.9	42.3	44.1
Cu	29.3	10.8	17.5	62.8	12.1	17.9	8.9	37.4	8.6	10.6	9.8	10.9	13.7	9.0
Nb	18.5	8.2	4.9	11.3	8.6	11.0	10.6	13.4	4.7	3.9	4.5	5.8	1.0	9.5
Zr	189.1	134.6	130.5	136.1	138.0	154.1	147.4	144.7	122.5	129.2	146.3	158.8	131.3	153.9

Element	11-6A	14-1A	12-2	1-2	15-3B	9-8B	9-9	9-12A	12-8	9-10	9-1	BR(this study)	BR(W.H.O.I. values)
Y	26.0	20.2	22.2	20.2	24.1	24.6	24.4	22.4	28.5	26.3	203.2	27.0	31.2
Sr	393.7	379.6	372.9	365.3	361.6	364.5	275.4	360.8	441.1	264.2	280.6	1408.0	1363.8
Rb	67.4	75.7	75.4	76.3	94.2	62.9	63.1	67.0	41.1	84.5	74.9	55.5	46.5
Ni	17.5	16.3	23.8	20.6	44.0	11.2	5.6	8.4	42.5	5.7	7.1	200.0	259.5
Cr	20.8	15.9	20.0	19.4	57.2	10.3	8.7	2.4	72.5	4.3	11.0	281.1	287.1
V	68.4	70.6	64.4	63.5	63.4	67.5	48.8	37.3	55.5	40.7	42.4	221.8	240.0
Co	10.8	8.2	9.2	8.3	11.4	7.5	4.3	4.7	9.7	5.4	7.9	56.4	56.2
Zn	43.6	42.8	50.5	37.2	40.2	33.9	37.0	38.0	41.0	52.3	30.1	147.4	135.1
Cu	9.2	17.6	37.7	8.4	4.6	1.8	11.4	0.0	16.6	40.3	2.3	76.1	80.0
Nb	3.7	10.7	5.1	10.0	12.8	5.3	4.9	5.8	7.8	4.5	0.0	126.7	114.7
Zr	142.5	149.7	129.8	135.2	140.3	126.0	105.4	130.7	143.9	106.2	108.3	299.8	251.1

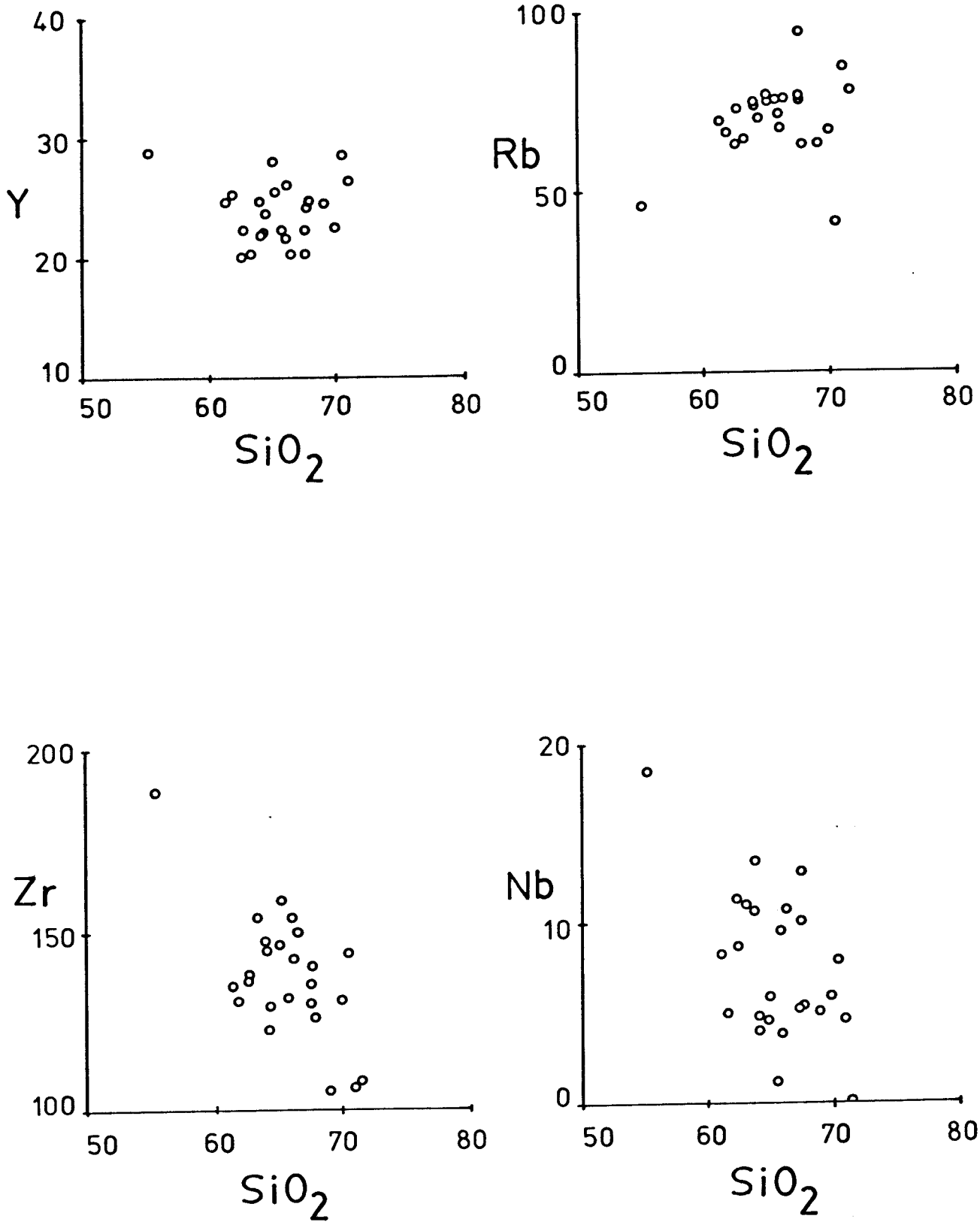

Figure 7 - Trace elements: Y, Rb, Zr, and Nb vs. SiO_2.

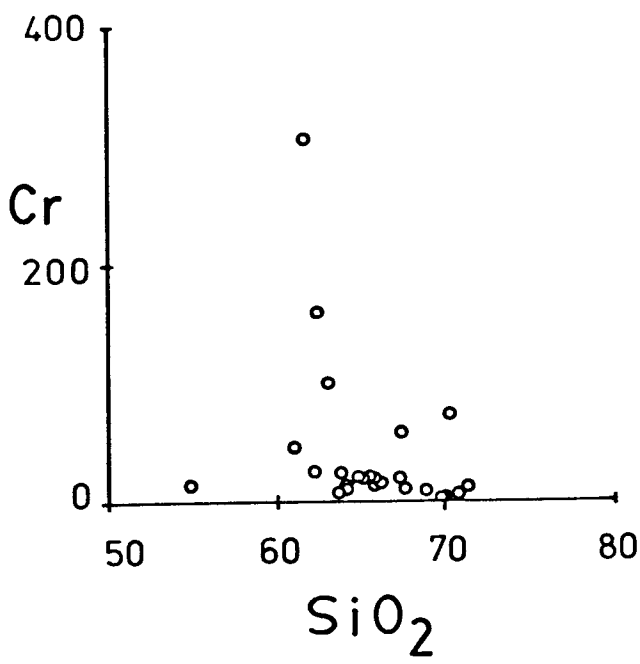

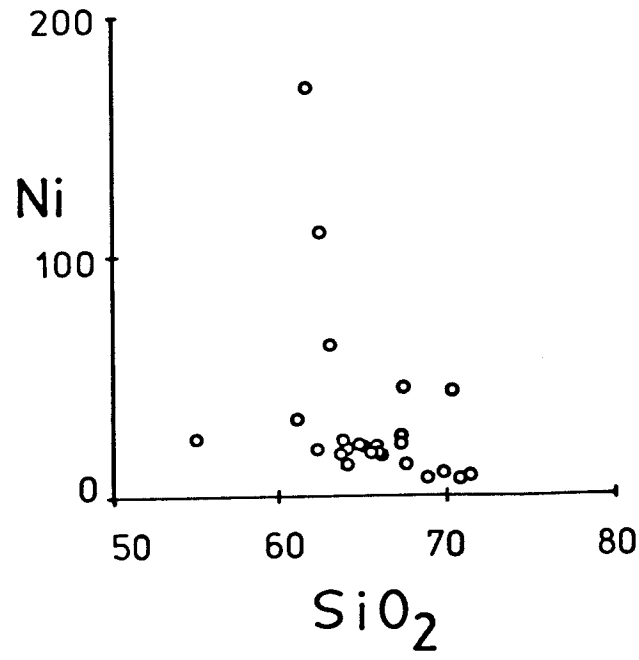

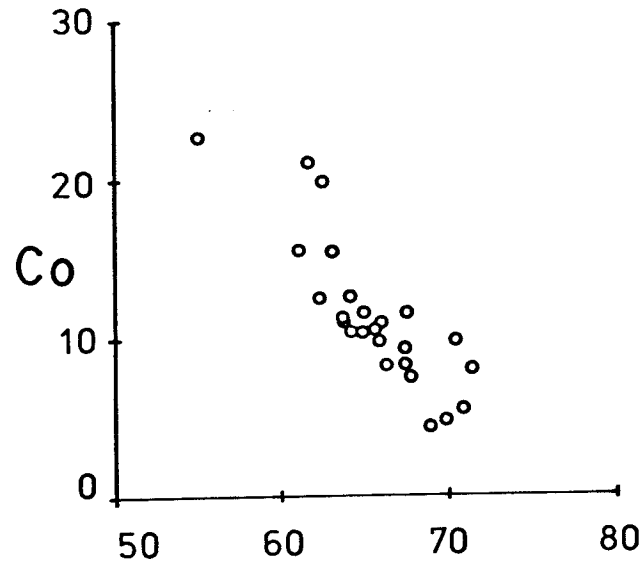

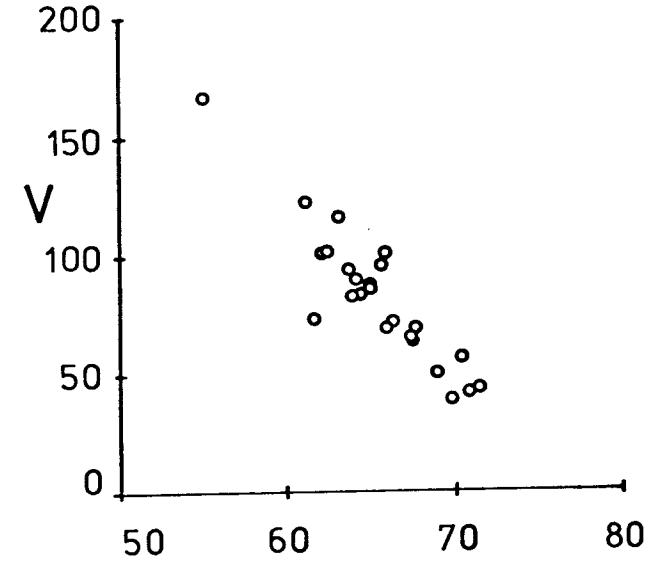

Figure 8 - Trace elements: Cr, Ni, Co, and V vs. SiO_2.

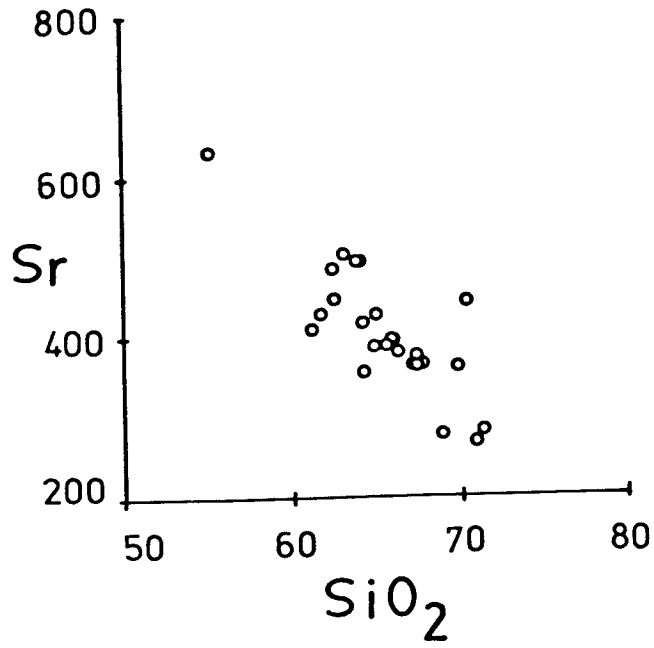

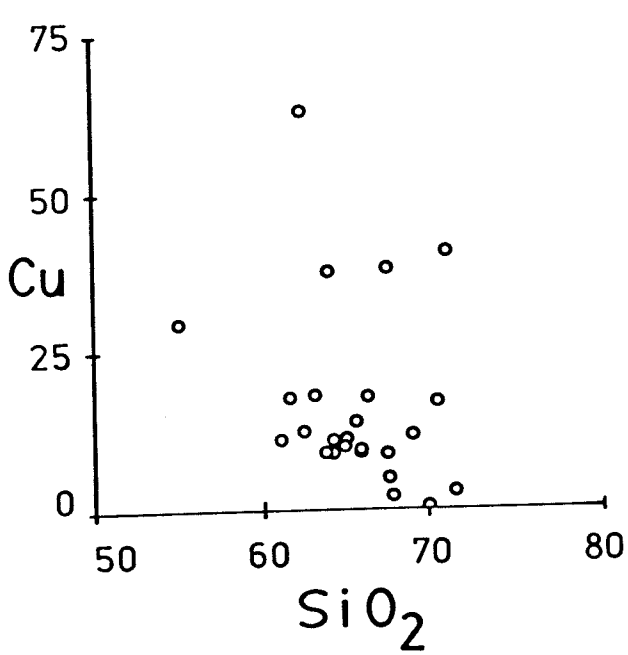

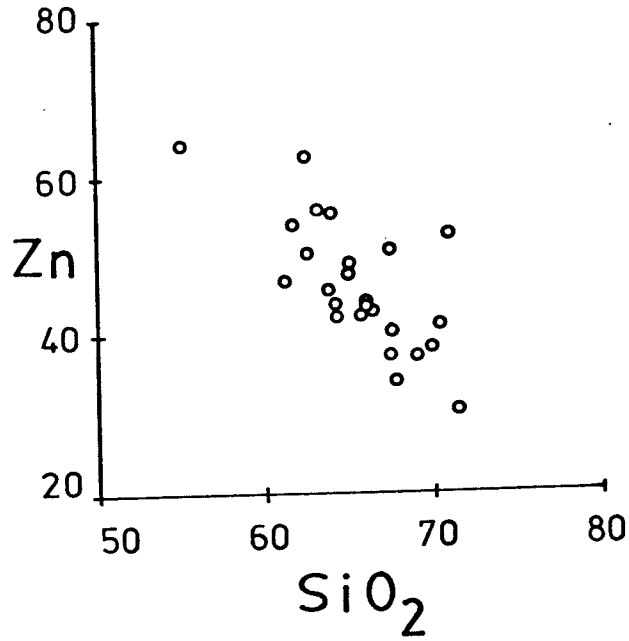

Figure 9 - Trace elements: Sr, Cu, and Zn vs. SiO_2.

a general decrease in abundances towards the most silicic members of the series, thus apparently behaving as compatible elements. Yttrium values remain roughly constant through the composition range of these rocks.

Strontium and the transition metals (Co, Ni, V, Cr, Cu, Zn) all show overall decreases in abundances in the Ankara rocks with an increase in silica (Figures 8 and 9). This is expected behavior for the compatible transition metals and certainly not unusual behavior for strontium. Transition metal abundances, particularly Ni and Cr, are significantly higher than the overall trend in some samples, particularly 7-4 and 8-4. Samples 22-10, 15-3B and 12-8 also have somewhat higher abundances of these elements.

Comparisons of trace element abundances in the Ankara volcanics with those in rock suites from other locations and tectonic settings are subject to the reservations about accuracy mentioned in the discussion of analytical techniques. Nevertheless, the abundances in the Ankara rocks are broadly comparable to volcanic rocks from active plate margins elsewhere. Ni/Co ratios, a sensitive indicator of tectonic setting (Bailey, 1981), of the andesites included in this study are similar to those of continental island arcs and Andean-type margins. A plot of K_2O vs. Rb values, also characteristic of tectonic setting of andesites (Bailey, 1981), again illustrates these affinities (Figure 10).

To summarize, as is the case with the major element data, the trace element data are generally fairly well correlated throughout the range of compositions in this rock suite. The trace element abundances are similar to those in other volcanics from active plate margins with continental basement, as are the major elements.

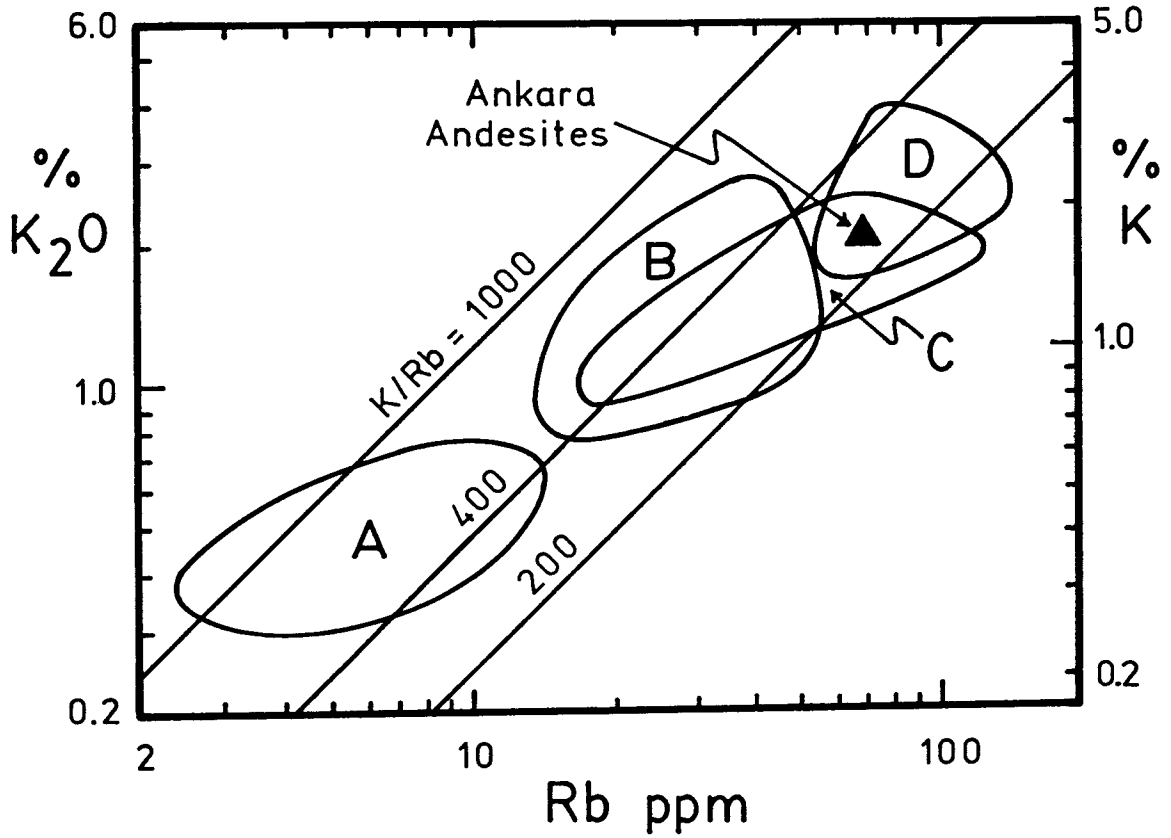

Figure 10 - Log K_2O vs. log Rb tectonic classification of andesites (after Bailey, 1981). A = low-K oceanic island arc andesites; B = other oceanic island arc andesites; C = continental island arc andesites and thin continental margins; D = Andean andesites. Solid triangle represents Ankara andesite average.

CHAPTER V

DISCUSSION

While the lavas of the Ankara volcanics exhibit a wide range in chemical composition, they do at the same time show a chemical consanguinity. That the process or processes leading to their formation are not necessarily simple ones is evidenced by the complicated phase relationships revealed in thin section. In this section, various processes will be discussed and evaluated as to their importance in the generation of these magmas. These processes include partial melting, fractional crystallization, and mixing/contamination effects. Finally, the relationship of this magmatism to regional tectonics will be evaluated.

Partial Melting

The process of partial melting can generate a suite of igneous rocks, and distinguishing this process from crystal fractionation is frequently difficult (Cox, et al., 1979). In the Ankara volcanics, the apparent change from incompatible to compatible behavior of Rb and K, usually incompatible elements, and the apparently compatible behavior of the normally incompatible elements, Zr and Nb place strong constaints on any petrogenetic model proposed for the origin and evolution of these rocks. Additional constraints are provided by bulk chemistries of the rocks.

In any partial melting process, incompatible elements will be enriched in the most silicic liquids, produced as the first increments of melting, and will decrease with increasing degrees of partial melting. (As an example, see Figure 14-1 in Cox, et al., 1979). This is

the behavior assumed in melting models of both mantle and crustal materials. Rubidium serves well as an example. It is incompatible in all major mantle phases composing pyrolite or peridotite source assemblages (although it could be contained in a minor phase such as phlogopite or kaersutite), and its behavior should be as expected in mantle-derived melts.

In melts derived from crustal materials the behavior of Rb will be expected to be similar, although for slightly different reasons. Biotite has a strong affinity for Rb, indicated by K_d biotite >>1 and is a common, although not major, crustal constituent. Experimental studies (Busch, et al., 1974) show that under anatectic conditions, biotite breaks down to form amphibole and pyroxene, enriching the melt in K_2O. This breakdown would also enrich the melt in Rb, since this element is incompatible in both amphibole and pyroxene. This element should therefore exhibit incompatible behavior in crustal melts. Even if this is not the precise mechanism of biotite breakdown, the incompatible behavior of Rb in rock suites apparently derived by partial melting of crustal materials (e.g. the Mormon Mt. volcanics of Arizona described by Gust (1981)), indicates that some similar mechanism probably must occur.

The expected trends resulting from incompatible behavior of Rb would be for the concentration to increase with increasing silica throughout the compositional range of the rock suite. The actual trend (Figure 7) is an increase of Rb from low to moderate SiO_2 content, followed by a levelling off or decline in the more silicic rocks. This difference between the expected and actual behavior of Rb suggests that partial melting is not the dominant process involved in the generation of this suite of rocks.

An examination of interelement relationships among trace elements casts further doubt upon this hypothesis. The use of trace elements to discriminate qualitatively among various petrogenetic processes is described in detail by Minster and Allegre (1978). In their discussion, they divide trace elements into groups of high, low, and intermediate solid/liquid partition coefficients. With the aid of various plots, they then use the differences in behavior among these groups of elements to discriminate between different petrogenetic processes.

This method can be applied with good results to the Ankara volcanics. The division of trace elements into Minster and Allegre's three groups is somewhat complicated by the variation in mineral K_d's with changing melt composition (e.g. Allegre et al., 1977) and by the effects of increased stability of minor phases, such as apatite and zircon, on D_{bulk}, the bulk distribution coefficient (e.g. Watson, 1979). Nevertheless, such a division can be made. Elements with high partition coefficients (compatible elements) include Ni, Cr, Co, and V. Those with moderate partition coefficients are Sr, Zr, Nb, and Y. For the purpose of constructing plots, K and Rb were considered to be elements with low partition coefficients (incompatible elements) despite the fact that they display incompatible behavior (increase with increasing SiO_2) only in the less silicic half of the suite (Figures 5 and 7). When the data for these elements are plotted on Minster and Allegre-type diagrams, the data from the more silicic samples fall on the trends defined by the data from the less silicic samples. The inclusion of all K and Rb data on the diagrams can therefore be justified.

The two plots that prove to be the most useful for the Ankara volcanics are those of log Cr vs. log Ni and K/Rb vs. Sr/Rb. On the

Cr vs. Ni plot, products of a melting process will plot near a single point, while products of fractional crystallization will plot along a positively sloping line with the most fractionated samples closest to the origin (Figure 11, inset). Products of a mixing/contamination process will plot between the endpoints of a positively sloping line segment. The values for the Ankara volcanics plot along a positively sloping line (Figure 11), indicating that fractional crystallization or possibly some mixing/contamination process, but not partial melting, best accounts for this suite of rocks.

A plot of K/Rb vs. Sr/Rb indicates that a hypothesis involving fractional crystallization best explains the observed variations in rock compositions (Figure 12). Products of a partial melting or mixing/contamination process should plot on lines, while those resulting from fractional crystallization should plot around a point (Figure 12, inset). The Ankara rocks have a very narrow range of both K/Rb and Sr/Rb values and plot in a cluster, corresponding most closely to the expected behavior of a rock suite derived by fractional crystallization. A hypothesis involving fractional crystallization will be more fully developed later.

Of course partial melting of some material must have produced a parental magma to this suite. Isotopic data are needed to confirm or deny any hypothesis concerning the ultimate source of these melts, and those data are unavailable for these rocks. However, some comments can still be made.

That any of the less differentiated rocks of the Ankara suite represent direct mantle partial melts is doubtful; experimental work has illustrated the difficulty in producing highly silicic melts from

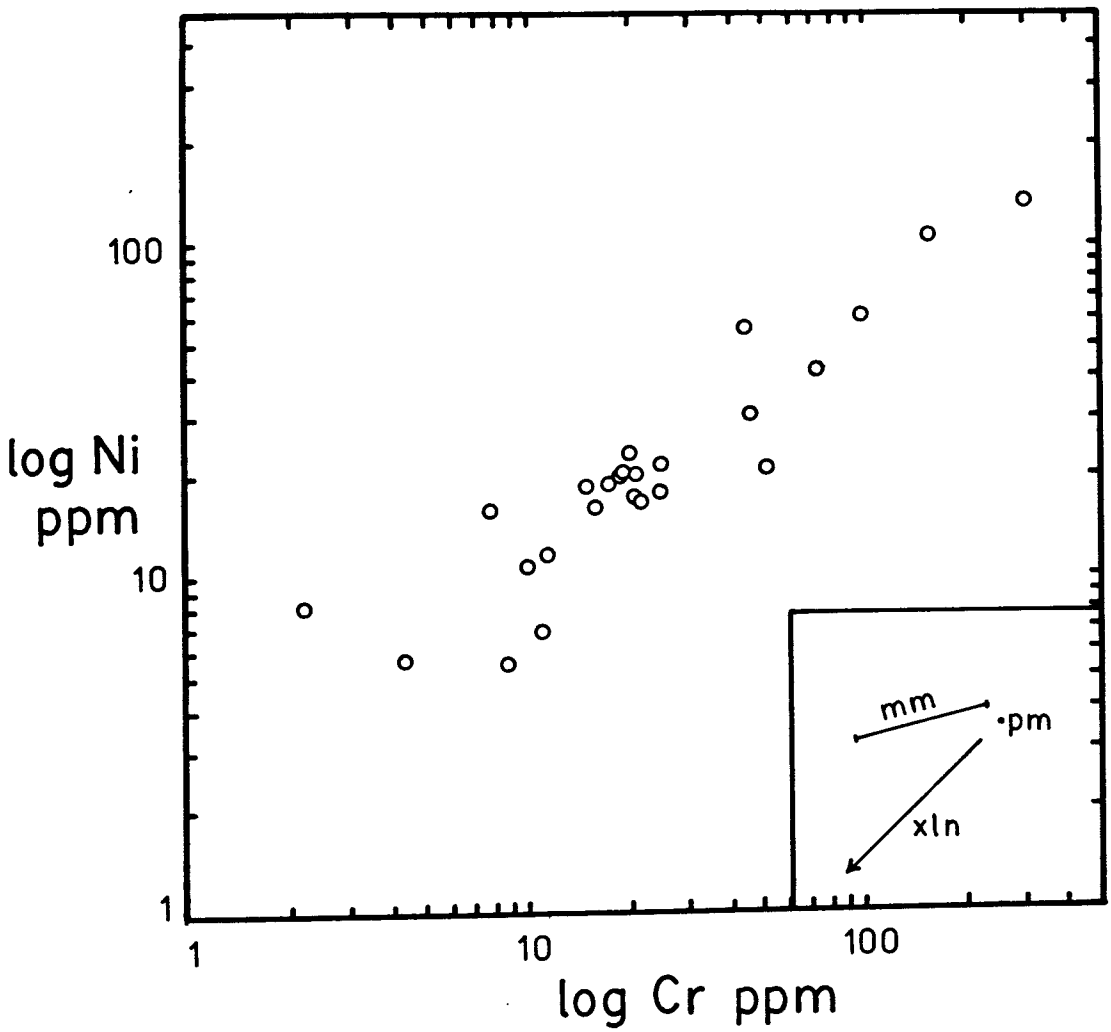

Figure 11 - Log Ni vs. log Cr for the Ankara volcanics. The inset shows qualitatively the behavior of trace elements in liquids (from Minster and Allegre, 1978). xln = fractional crystalization, pm = partial melting, mm = magma mixing.

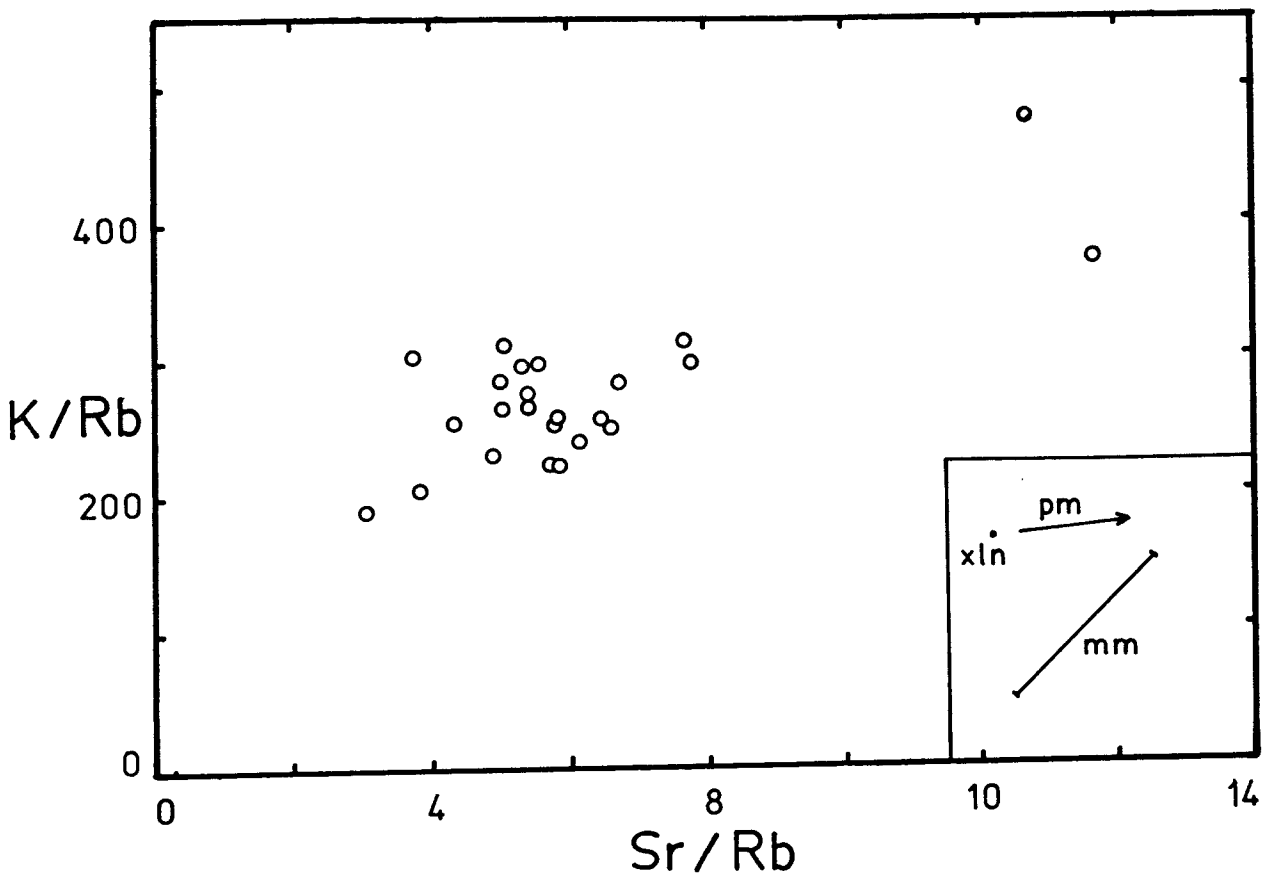

Figure 12 - K/Rb vs. Sr/Rb for the Ankara Volcanics. The inset shows qualitatively the behavior of trace elements in liquids (from Minster and Allegre, 1978). xln = fractional crystalization, pm = partial melting, mm = magma mixing.

mantle sources (Ringwood, 1977). The low concentrations of such compatible elements as Ni and Cr cast further doubt on a direct mantle origin for any of the less evolved members of this suite. If they are indeed mantle products, though, these melts must then represent magmas which have already been subjected to some sort of fractionation. This fractionation may have been similar to the olivine + chrome spinel fractionation (< 15%) proposed by Nichols and Whitford (1976) to produce melts with low Ni and Cr values and Mg numbers less than 60 in the Sunda Arc. Forsteritic olivine in the least silicic sample may be some indication of such a process.

Partial melting of amphibolitic lower crust could also produce a parental Ankara melt; this explanation is less complex than the preceding one, and is perhaps more plausible. Gust (1981) makes a strong case for the calc-alkaline rocks of the Mormon Mt. volcanic field, Arizona, representing different degrees of partial melting of such material. Major element concentrations of the Mormon Mt. rocks are very similar to those of the Ankara volcanics. By analogy to the Mormon Mt. suite, the Ankara parental magmas may have been generated in that fashion, even though trace element relationships preclude the derivation of the entire suite by this process.

Melts of approximately dacitic to rhyodacitic composition have been produced experimentally by smaller degrees of partial melting than those that produce andesites (Helz, 1976). A comparison of Helz's experimental liquid compositions and the compositions of the Ankara volcanics, when plotted on a Qz-Ab-Or ternary diagram, illustrates the similarities between the liquids and rocks, providing support to the idea of a crustal derivation of these rocks (Figure 13).

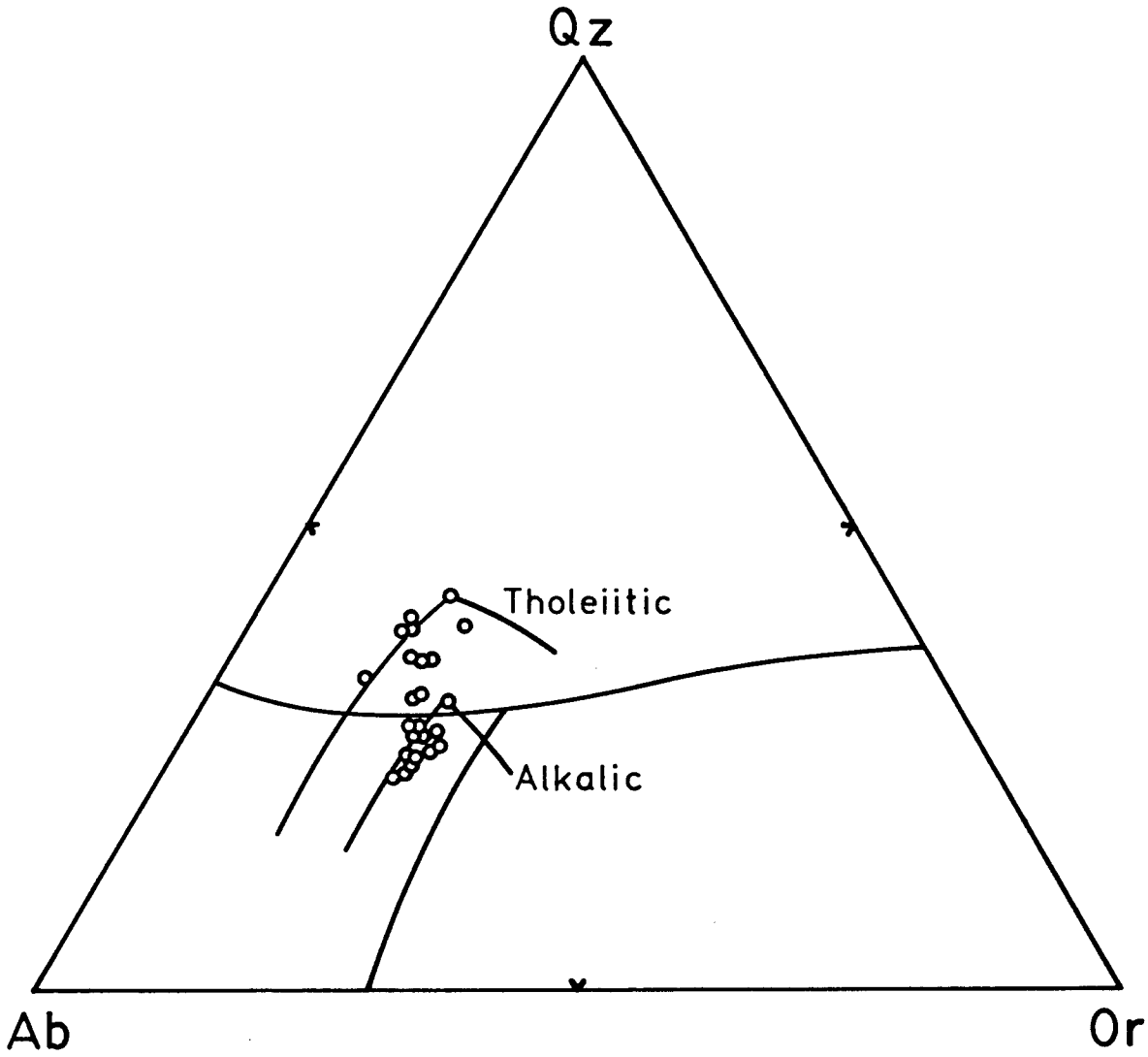

Figure 13 - Normative Qz-Ab-Or ternary diagram showing compositions of the Ankara volcanics. The trends of Helz's (1976) experimental melts are indicated.

In summary, although partial melting must have generated an initial parent magma to the Ankara volcanics, a petrogenetic model relying solely on variation in degrees of partial melting cannot explain the observed chemical trends in these rocks.

Fractional Crystallization

The process of fractional crystallization is widely applied to explain the chemical evolution of suites of volcanic rocks (Cox, et al., 1979) and, as stated in the previous section, this process was undoubtedly the dominant one involved in the generation of the various magmas represented in the Ankara region. The additional evidence for the operation of this mechanism will be examined in this section, first qualitatively, then quantitatively.

Qualitative observations supporting a fractional crystallization hypothesis for the origin of these lavas include both the petrography and the general chemical trends. The consistent occurrence of the assemblage plagioclase + hornblende + biotite + Fe/Ti oxides as both the phenocryst assemblage and the constituents of glomeroporphyritic clots suggests that these phases are the ones which play a dominant role in crystal fractionation. The pyroxenes may contribute in a smaller capacity. This conclusion is supported by the proposed fractionation of these phases in volcanic suites from other calc-alkaline margins (Arculus and Wills, 1980).

To check this hypothesis with major element chemistry, several two-element variation diagrams were constructed with the compositions of the Ankara plots plotted on them. Vectors representing the removal of various amounts of individual mineral phases from a starting

composition of sample 22-10 were then constructed. With the aid of such diagrams, the relative importance of the various possible fractionating phases can be evaluated. Examples of these diagrams are presented in Figures 14 and 15.

The least silicic sample, sample 2-4, was not used as a parent magma for the calculations due to its MgO content and Mg number, which are very low for its SiO_2 content. This disequilibrium assemblage of forsteritic olivine and quartz, a possible indication of a contamination/mixing process, also argued against its use. Similar reasons precluded the use of sample 11-9, and samples 7-4 and 8-4 were eliminated on the basis of their very high trace transition metal abundances. Sample 21-5 was analyzed by J.M. Dyer for trace elements under different machine conditions and was eliminated for this reason. This left sample 22-10 as the next candidate for use as a parent, and this sample was chosen to serve in that capacity. Its slightly high trace transition metal abundances were adjusted somewhat when used for trace element modelling (Figure 19).

Figure 14 plots alumina against lime and illustrates both the importance of plagioclase in the control of these two elements and the large fraction of this mineral which must have fractionated during the evolution of these magmas. Similarly, Figure 15 indicates that titanomagnetite must have played a role in the fractional crystallization of these melts, although a large quantity of this phase need not have been removed. The pure magnetite (no Ti component) vector (not shown) lies above the rock trend, indicating that this phase must have had a titaniferous component. This diagram also indicates that hornblende and/or biotite were important fractionating phases. The importance

Figure 14 - Major element modelling on an Al_2O_3 vs. CaO diagram. Solid lines are mineral subtraction vectors. Dashed line represents the trend of Models I and II. Open circles are the compositions of the Ankara volcanics. Error bars are 5%.

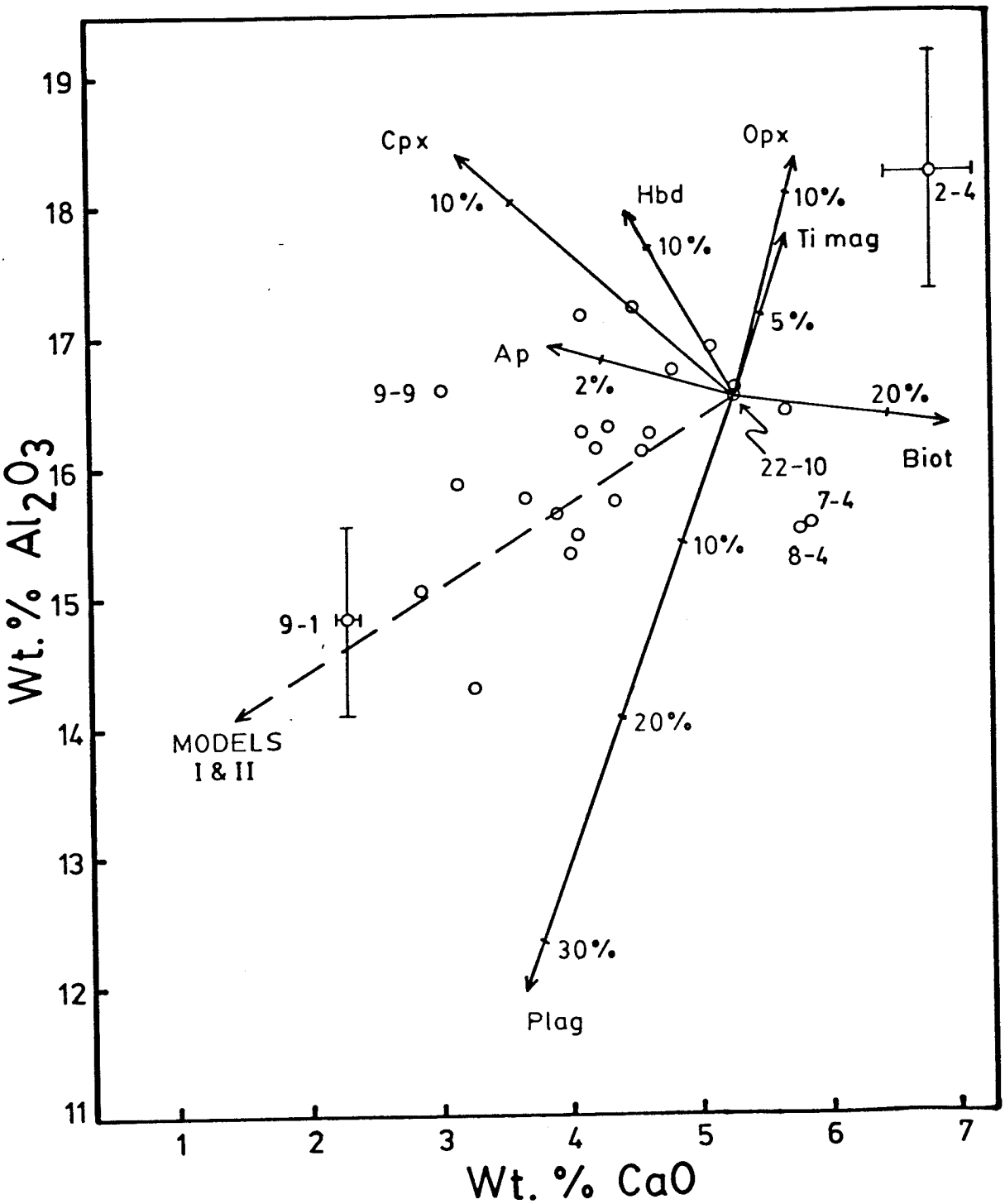
Wt.% Al_2O_3
Wt. % CaO
19
18
17
16
15
14
13
12
11
1
2
3
4
5
6
7
Cpx
10%
Hbd
10%
Opx
10%
Ti mag
5%
2-4
Ap
2%
9-9
20%
Biot
22-10
7-4
8-4
10%
9-1
MODELS
I & II
20%
30%
Plag

Figure 15 - Major element modelling with a TiO_2 vs. FeO* diagram. Symbols are the same as in Figure 14.

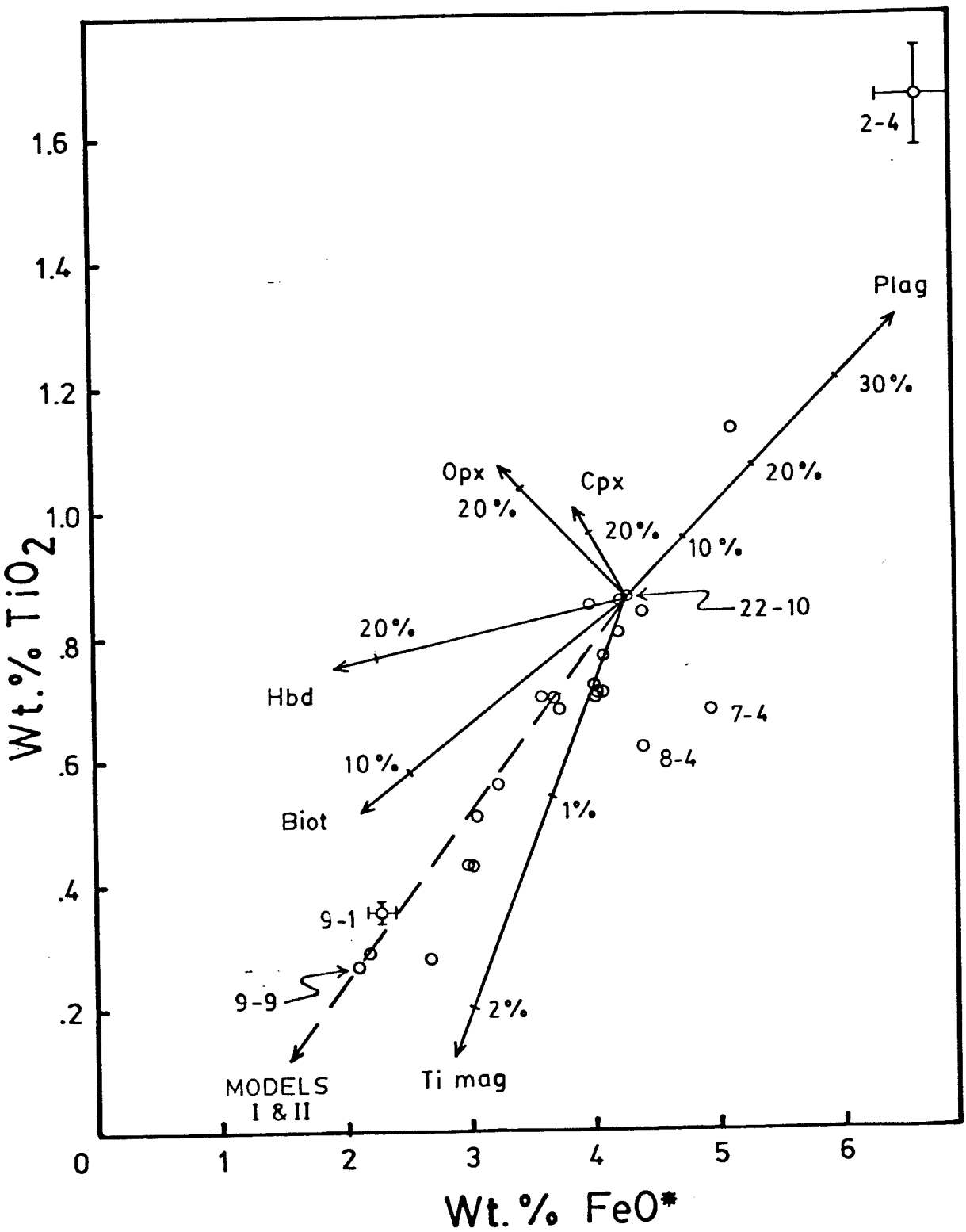
2-4
Plag
30%
20%
Opx
20%
Cpx
20%
10%
22-10
20%
Hbd
10%
Biot
7-4
8-4
1%
9-1
9-9
2%
MODELS
I & II
Ti mag
Wt.% TiO2
Wt.% FeO*
1.6
1.4
1.2
1.0
.8
.6
.4
.2
0
1
2
3
4
5
6

of biotite as a fractionating mineral is confirmed by consideration of K_2O variation within this suite (e.g. Figure 5). Potash content does decrease in the more silicic compositions, and because biotite is the only significant potassium-bearing mineral in these rocks (the amphiboles present contain only 0.1 to 0.3% K_2O), this variation must be under biotite control.

Trace element trends (Figures 7, 8 and 9) tend to confirm these ideas. Plagioclase is the only mineral which has a partition coefficient greater than unity for Sr, so that the observed decrease in Sr content toward the more acid members may be ascribed solely to the fractionation of this phase. This same observation holds true for Rb and biotite.

Relations between the other trace elements and possible fractionating phases are not so distinct, because frequently for a given element two or more phases exhibit similar partition coefficients greater than one. Consequently, control of the concentration of that particular element cannot be uniquely related to the fractionation of one particular phase. As an example, Nb exhibits large, similar K_d's for hornblende, biotite, and magnetite in acid melts (4.0, 3.0, and 2.5 (Pearce and Norry, 1979)). Thus, the fractionation of enough of any of these phases individually or in combination could lead to the observed Nb decrease in more silic rocks, as long as $D_{bulk} > 1$. This behavior for Nb and similar behavior for Zr (which is incompatible in magnetite) was used by Pearce and Norry (1979) to indicate the importance of fractionation of hornblende + biotite and zircon in the volcanics of Andean-type margins and to distinguish those rocks from others from other types of active plate margins.

Further complications are introduced by the minor phases zircon and apatite, common minor phases in these rocks. The possible major importance of these phases in control of particular trace elements is discussed by Watson (1979), Hanson (1978), and Fourcade and Allegre (1981).

The hypothesis of derivation of this range of magmas through the process of fractional crystallization was tested more rigorously through the use of major element mixing calculations, and was checked by trace element modelling. The methods of the calculations employed are given in Appendix IV. The results of these calculations can be considered as only semi-quantitative, because only a few mineral analyses are available for this rock suite and these analyses are confined to just a few samples. It is therefore not possible to take into account changes in mineral chemistry of the fractionating phases as the melt evolves. For some phases, i.e. biotite and the opaque phase, no analyses are available at all. For these cases, a published analysis of a biotite from a tonalite was used (Table 4), and the opaque was assumed to be a pure titanomagnetite of a composition which was calculated to fit the model well. Mineral compositions used in these mixing calculations are given in Table 4.

Trace element calculations suffer from the wide range of published distribution coefficients for intermediate to acid melts (Arth, 1976; Gill, 1978; Allegre, et al., 1977). This range is due, in part, to the variation of a given K_d with changing melt composition (Fourcade and Allegre, 1981); this phenomenon also adds a further complication to the calculations. Distribution coefficients used in this study and their sources are listed in Table 5.

TABLE 4:

MINERAL COMPOSITIONS USED IN MAJOR ELEMENT MODELLING

Oxide	An_{40} (1)	Opx (1)	Cpx (1)	Hbd (1)	Biot (2)	Ap (3)
SiO_2	58.62	56.22	52.71	49.34	36.67	--
TiO_2	0.03	0.13	0.45	1.29	3.39	--
Al_2O_3	25.72	1.61	3.06	6.00	17.10	--
FeO	0.25	7.68	5.53	11.82	20.11	--
MnO	0.02	0.17	0.17	0.41	0.04	--
MgO	0.00	31.82	17.50	15.65	9.20	--
CaO	8.54	1.65	20.74	11.07	0.38	56.84
Na_2O	6.30	0.03	0.38	1.32	0.21	--
K_2O	0.44	0.02	0.05	0.35	9.17	--
Cr_2O_3	0.00	0.52	0.42	0.00	0.00	--
Total	99.92	99.85	101.01	97.25	96.81	56.84

(1) result of microprobe analysis from this study

(2) published analysis for a biotite from a tonalite (Deer, Howie, and Zussman, 1962)

(3) calculated from stoichometric composition

TABLE 5:

MINERAL Kd'S USED IN TRACE ELEMENT CALCULATIONS

	Plag	Hbd	Biot	Cpx	Mgt
Sr	2.84(1)	.33(2)	--	.02(2)	--
Rb	.07(2)	.05(2)	4.1(4)	.02(2)	--
Ni	--	2(4)	12(3)	3.5(3)	12(3)
Co	--	5(4)	6(4)	1(4)	5(4)
Cr	--	5(4)	5(4)	8(4)	15(3)
V	--	5(4)	8(4)	0.7(4)	20(4)

(1) Arth (1976), dacite value

(2) Gill (1978), recommended value

(3) Gill (1978), within suggested range

(4) estimate, considering bulk composition and relative values among elements; based on published values with suggestions from J.F. Bender (pers. comm.).

Three major element models are presented in Figures 16, 17 and 18, hereafter referred to as Models I, II, and III. The first two have a composition similar to sample 9-1 as their final composition and differ essentially only in the fact that Model I contains clinopyroxene while Model II contains orthopyroxene. Both these models are within the experimental error (5%) in the analysis of sample 9-1. Trace element calculations for Model I employing Rayleigh fractionation are in basic agreement with the major element calculations (Figure 19). The conclusions that can be drawn from these models are that:

1) plagioclase is the dominant fractionating phase (26% removed);
2) biotite and hornblende are the dominant mafic phases (8% and 6% removed, respectively);
3) ortho- or clinopyroxene or a combination of the two plays a minor role in fractionation (< 3% removed); and
4) a small amount of an Fe-Ti oxide phase (< 1%) is involved in the fractionation.

The total quantity of solids removed is 44% in these models.

In Figure 20, rock compositions are again plotted on a K_2O vs. SiO_2 variation diagram, along with various modelled trends. On this diagram, it can be seen that with the exception of sample 9-1, the general trend is for K_2O to first increase with increasing SiO_2, then, after 64-65% SiO_2, to decrease with increasing silica. Because biotite is the only mineral phase present with an appreciable K_2O content (the amphiboles present contain only 0.1 to 0.3% K_2O (Appendix III)), the decrease in K_2O content of the more fractionated rocks can be ascribed solely to the removal of biotite. Model III (Figure 18) was calculated

Figure 16 - Major element modelling: Model I

100 Extract = 59 An_{40}: 17 Biot: 12 Hbd: 8 Cpx: 2 Fe/Ti oxide (67:33 Fe:Ti): 2 Ap

44% removed

	Initial Composition (22-10)	Calculated Final Composition	Expected Final Composition* (9-1)
SiO_2	63.05	72.51	71.34 ± 3.6
TiO_2	0.86	0.37	0.37 ± .02
Al_2O_3	16.52	14.52	14.84 ± .74
FeO	4.29	2.33	2.29 ± .12
MgO	0.02	-0.03	0.01
CaO	5.31	2.35	2.31 ± .12
Na_2O	3.91	3.88	3.89 ± .19
K_2O	2.29	2.63	2.71 ± .14

* 5% error indicated

Figure 17 - Major Element modelling: Model II

100 Extract = 60 An_{40}: 17 Biot: 12 Hbd: 4 Opx: 2 Fe/Ti oxide (65:35 Fe:Ti): 4 Ap

44% removed

	Initial Composition (22-10)	Calculated Final Composition	Expected Final Composition* (9-1)
SiO_2	63.05	73.44	71.34 ± 3.6
TiO_2	0.86	0.37	0.37 ± .02
Al_2O_3	16.52	14.48	14.84 ± .74
FeO	4.29	2.33	2.29 ± .12
MnO	0.02	0.01	0.01
CaO	5.31	2.38	2.31 ± .12
Na_2O	3.91	3.86	3.89 ± .19
K_2O	2.29	2.63	2.71 ± .14

* 5% error indicated

Figure 18 - Major element modelling: Model III

100 Extract = 50 An_{40}: 30 Biot: 10 Hbd: 6 Cpx: 1 Fe/Ti oxide (48:52 Fe:Ti): 4 Ap

37% removed

	Initial Composition (22-10)	Calculated Final Composition	Expected Final Composition* (9-9)
SiO_2	63.05	71.65	68.88 ± 3.4
TiO_2	0.86	0.27	0.27 ± .01
Al_2O_3	16.52	15.20	16.58 ± .83
FeO	4.29	1.95	2.09 ± .10
MnO	0.02	-0.01	0.02
MgO	2.39	0.61	0.57 ± .03
CaO	5.31	3.03	3.04 ± .15
Na_2O	3.91	4.23	4.12 ± .21
K_2O	2.29	1.87	1.94 ± .10

* 5% error indicated

Figure 19 - Trace element calculations: Results of a Rayleigh fractionation model* applied to Model I

Element	C_0 (22-10)**	D_{bulk}	C_L (9-1)	F, calculated
Sr	445	1.73	280.6	0.532
Rb	64.5	0.75	74.9	0.550
Ni	21	2.80	7.1	0.547
Co	13	1.80	7.9	0.537
Cr	25	2.39	11.0	0.550
V	100	2.42	42.4	0.546

* $C_L/C_0 = F^{(D-1)}$

** Values are slightly adjusted so that they fall on overall trends. (see Table 3 for a comparison with actual values.)

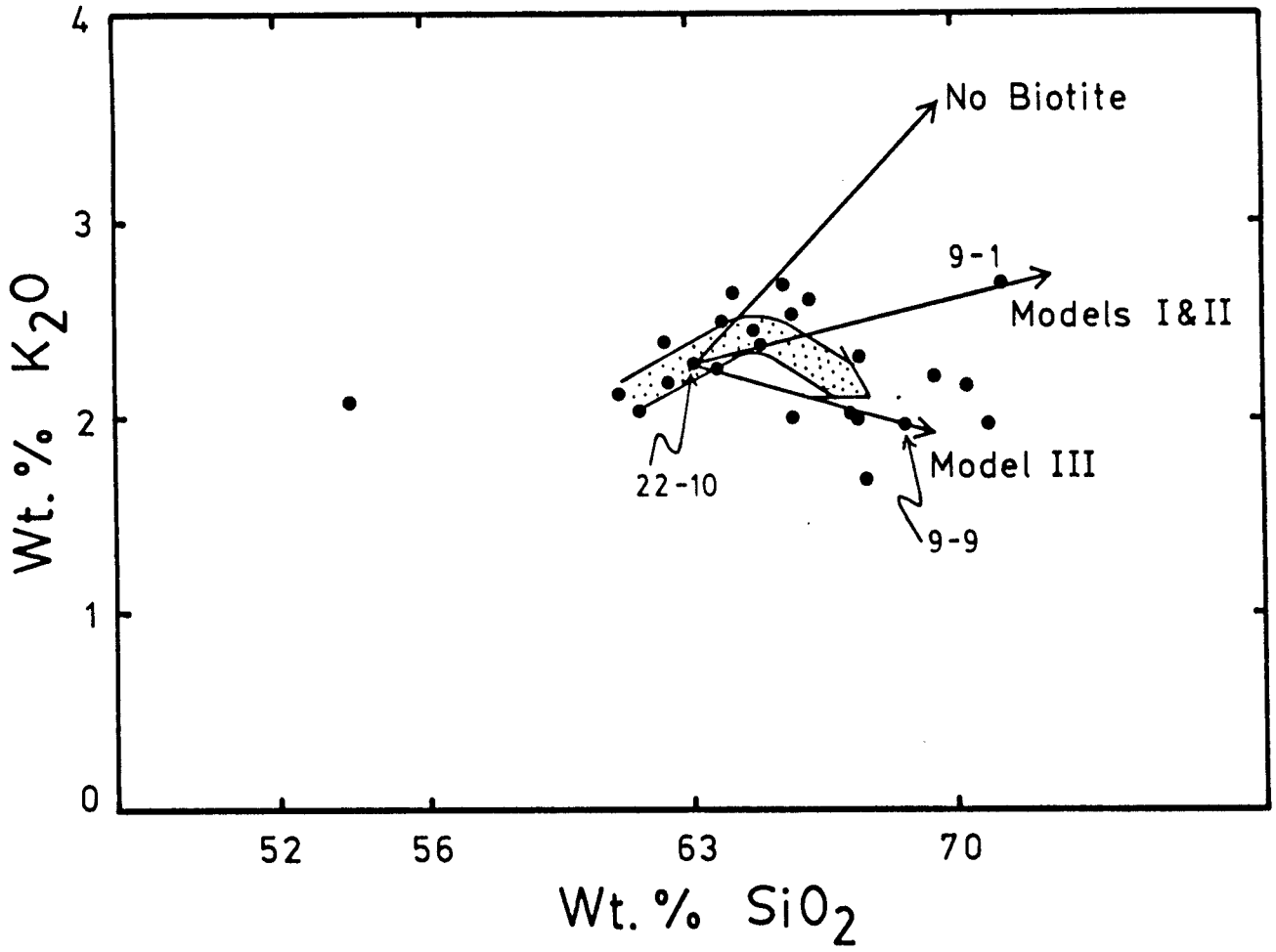

Figure 20 - K_2O vs. SiO_2 diagram indicating the trends of various fractionation models. The importance of biotite as a fractionating phase is readily apparent (Model III).

to determine the amount of biotite needed to be fractionated from sample 22-10 in order to derive sample 9-9. Other phases involved in fractionation were left in the same relative ratios as in Models I and II so that the models would reflect only differences in the degree of biotite fractionation. That Model III approaches the composition of sample 9-9 so closely is a strong indication that the degree of biotite fractionation is indeed the primary reason for the difference between sample 9-1 and those similar to 9-9. Rather than postulating two distinct fractionation trends, however, a more reasonable and consistent explanation (given the close correlation of all other elements) is that sample 9-1 represents a rock which has been enriched in biotite. A simple calculation reveals that only about 5% biotite needs to be added to its closest neighbors in Figure 20 to produce sample 9-1 from them. This explanation is therefore quite plausible chemically. Estimates of modal biotite in sample 9-1 are similar to those of the other more silicic rocks in this suite (Table 1), and so petrography does not necessarily support this conclusion. However, such a small increase in modal biotite certainly falls within the range of error involved in making such estimates, and so could easily escape detection.

Possible mechanisms for the removal of biotite from a melt (and so for the enrichment of the fractionating assemblage) include filter pressing and crystal flotation. Any hypothesis concerning such a mechanism will be based on textural relations. The number of broken phenocrysts present indicate a violent history for sample 9-1, and any textures indicative of a biotite removal mechanism have undoubtedly been destroyed. Thus there is little basis for favoring any particular biotite removal mechanism in these rocks.

To summarize this section, abundant evidence both petrographic and especially chemical, points to fractional crystallization as the major mechanism in producing the range of magmas represented in the Ankara volcanics. Plagioclase is the dominant fractionating phase, while, in order of decreasing importance, biotite, hornblende, orthopyroxene and/or clinopyroxene, and opaques also play a role in fractionation. The relative ratios of these phases remain similar throughout fractionation, with the exception of biotite, which plays an increased role in the fractionating assemblages at silica contents greater than about 66%. One high silica sample may have been enriched in biotite relative to the others, presumably by the same mechanism which removes biotite from the magma.

Mixing and Contamination Processes

The idea of producing lavas of intermediate composition by the mixing of basaltic and rhyolitic end members has been considered over a period of quite some time by various authors (Bunsen, 1851, Curtis, 1968; Eichelberger, 1975, 1978). As indicated in the discussion of partial melting, the discrepancies between the observed chemical compositions and trends of the more silicic Ankara volcanic rocks and those expected of crustal partial melts rule out the derivation of those rocks by the process of partial melting of crustal material. Because in such a mixing model, the most silicic rocks are similar in composition to crustal melts (Eichelberger, 1978) and the corresponding Ankara rocks are not, this process can be ruled out in this case. The trace element relationships described in the partial melting discussion (i.e. Figures 11 and 12) also rule out large scale

mixing of discrete magmas, as was previously stated.

Smaller scale mixing/contamination processes have undoubtedly had some influence on at least some of the Ankara rocks, however. Disequilibrium mineral assemblages, reaction relations between phases or a phase and the melt, resorption of phases, and complex zoning and dendritic growth in feldspars all give evidence that some mixing or contamination of some kind may have occurred.

As mentioned in the petrography section, xenocrystal phases are probably present in some samples. The low silica content, presence of forsteritic olivine, and reaction rims of clinopyroxene around them, indicate that the quartz grains in sample 2-4 are most likely xenocrysts. Quartz in other samples (7-4 and 8-4) exhibits similar rims and the round clusters of acicular clinopyroxene found in samples 8-4 and 11-9 may represent a quartz + melt → clinopyroxene reaction carried to completion (Eichelberger, 1978). Quartz in all of these rocks may also be xenocrystic. Xenocrystic quartz may have been either picked up from the country rock or may be evidence of mixing of a quartz-bearing Ankara magma with a less silicic one.

Eichelberger (1978) ascribes the embayed grain shapes of quartz, nearly universal in intermediate volcanic rocks, to magma mixing. Other authors (Green and Ringwood, 1968) consider resorbed quartz to be a product of pressure change as the magma rises. The euhedral shape, with only slight embayments, of quartz grains in sample 15-9 indicates that at least some of the quartz in these rocks first crystallized from the melt, then was later resorbed by it. The Green and Ringwood interpretation may then hold true for the embayed quartz in the Ankara rocks, especially in the more silicic samples.

Xenocrystal origin of pyroxene clots in samples 7-4 and 8-4 was also postulated in the petrography section. In this case, chemical evidence may be used to confirm this supposition. A glance at Figures 14 and 15, which illustrate the effect of fractionation of different minerals in terms of major elements, reveals that those samples lie off the general trend. They can be related to that trend by back-projection along the ortho- and/or clinopyroxene fractionation trends. This can be interpreted to indicate addition of these phases to a rock composition lying on the general trend. This interpretation is also consistent with the observed high trace transition metal (Ni, Cr, Co) abundances in these samples. The chromian nature of the pyroxenes was noted previously, and it can be assumed that a chromian pyroxene would be enriched in other transition metals of similar chemical behavior. Thus all chemical evidence supports xenocrystal origin of the pyroxenes in these two rocks; this argument may also be applied to the other samples containing smaller amounts of pyroxene and showing lesser transition metal enrichment relative to the general trend. Textural relationship of the pyroxenes suggest that they represent a cumulate assemblage, while the high magnesia, alumina, and chrome contents of both the orthopyroxenes and the clinopyroxenes (Appendix III) indicate that this cumulate assemblage is from a much more basic magma of mantle derivation.

The plagioclase phenocrysts present in the Ankara volcanics exhibit many signs of disequilibrium conditions during their growth. These include discontinuous and oscillatory zoning, zones of dendritic growth, rounded or corroded grain margins, and grains consisting of rounded, more sodic(?) cores with euhedral overgrowths. The origin

of calcic and complexly zoned feldspars has been ascribed to crystallization under high P_{H_2O} (Arculus and Wills, 1980 and others), the accidental inclusion of xenocrystal material (Gust and Johnson, 1981 and others), or the mixing of magmas (Anderson, 1976; Eichelberger, 1978; Hibbard, 1981; and others). Plagioclase phenocrysts with the features noted above are characteristic of calc-alkaline lavas (Garcia and Jacobson, 1979), so it is preferable that any explanation of these phenomena be universally applicable to calc-alkaline suites. The xenocrystal origin hypothesis suffers in this regard, because the origin of the plagioclase is then explained as a chance phenomenon. The crystallization of calc-alkaline magmas under hydrous conditions has not been shown to occur universally; some suites may have crystallized under conditions of relatively low P_{H_2O} (e.g. Banner, 1981). Thus this mechanism may not be universally applicable as an explanation of the plagioclase phenomenon either.

Banner (1981) argues convincingly for precipitation of plagioclase from a mafic magma and subsequent mixing of that plagioclase (with or without its enclosing magma) with a more silicic melt as the probable origin of the observed plagioclase features. This idea enjoys universal applicability to calc-alkaline suites as it is independent of the conditions of crystallization. The nearly universal occurrence of other phases out of equilibrium with their enclosing melt in these rock types (Eichelberger, 1978) supports this idea.

The Ankara rocks too have other phases present which are out of equilibrium, such as the previously described quartz, orthopyroxene, and clinopyroxene xenocrysts. These, along with the plagioclase, phenomena, could be interpreted as petrographic evidence of some sort of wholesale mixing of a basic and an acid magma, as proposed by Eichel-

berger (1978) to explain the origin of intermediate to silicic magmas. However, as stated previously, the chemical evidence strongly supports a derivation of the Ankara magmas through the process of fractional crystallization and does not support a large-scale magma mixing hypothesis for their origin.

The various plagioclase phenomena and the frequent presence of xenocrystic phases in the rocks studied may well indicate a disequilibrium process of a smaller scale, though. Magma chambers may very well be compositionally inhomogeneous; the existence of zoned magma chambers has even been suggested, with zoned eruptive sequences being offered as supporting evidence (Cox et. al., 1979). Small amounts of convective mixing within an inhomogeneous magma chamber could provide large enough changes in the physico-chemical environment of phenocrysts to produce the observed disequilibrium features; large-scale mixing of two discreet magma types is not necessarily needed to produce them. The consistancy of composition of such phases as hornblende and biotite throughout this rock suite (as evidenced by optical properties), coupled with the varying degrees of resorption and reaction exhibited by these phases, even within the same thin section, argues for this explanation.

Disequilibrium processes, then, have undoubtedly played some role in the production of the observed phenocryst features. However, bulk chemical constraints rule out the large-scale mixture of two widely differing magma types. The observed disequilibrium features can most probably be related to small-scale convective mixing occurring within an imhomogeneous magma chamber.

The Relationship of Magmatism to Regional Tectonics

The chemical evidence amassed in this study indicates that the rocks of the Ankara volcanics are typical of those found in magmatic arcs built upon continental basement in either island arc or active continental margin settings. This is consistent with the occurrence of these volcanics on Cimmerian basement. These rocks are therefore considered to be the result of a Middle Eocene subduction zone related to the convergence that finally closed the Izmir-Ankara Ocean and the northern branch of Neo-Tethys, as described by Şëngör and Yilmaz (1981). Knowledge of the geometry of this arc relative to either of these oceans must await the detailed structural mapping needed in this area to elucidate the relationships between the small continental blocks and their corresponding suture zones that comprise this portion of Anatolia.

The exact relationship between the Ankara volcanics and the Ankara mélange is as yet also uncertain. Detailed mapping should clarify this relationship too. The volcanic unconformably overlie Paleozoic greywackes to the south, but apparently overlie rocks of the Ankara mélange to the north. If mapping reveals that the volcanics do lie entirely upon mélange, then it is somewhat doubtful that they are arc-related; they then may represent melts produced following the collision which closed the small ocean basins mentioned above.

CHAPTER VI

CONCLUSIONS

The results of this study lead to the following conclusions:

1) The Ankara volcanics consist of a Middle Eocene suite of rocks in the series basaltic andesite - andesite - dacite - rhyolite. They are moderately to highly porphyritic, with plagioclase the dominant phenocryst phase. Hornblende, biotite, quartz, and Fe/Ti oxides are present in most samples, and orthopyroxene and clinopyroxene in some.

2) Major and trace elements show generally clear trends throughout the suite. These trends can best be explained petrogenetically by invoking fractional crystallization of the observed phenocryst phases.

3) Diverse textures among the phenocryst phases suggest that disequilibrium processes also played at least a minor role in the development of these magmas. Convective mixing within an inhomogeneous magma chamber might explain these textures best.

4) Both the bulk chemistries of these rocks and their major and trace element trends suggest that the Ankara volcanics are the products of subduction-related volcanism erupted onto continental basement. This interpretation is broadly consistent with current tectonic models, but the determination of the exact relationship of these rocks to those models must await more detailed studies of the structural geology of the

region.

BIBLIOGRAPHY

Albee, A.L., and Ray, L., 1970. Correction Factors for Electron Probe Microanalysis of Silicates, Oxides, Carbonates, Phosphates, and Sulfates. Anal. Chem., 42: 1408-1414.

Allegre, C.J., Treuil, M., Minster, J.F., Minster, B., Albarede, F., 1977. Systematic use of trace elements in igneous processes - Part I: Fractional crystallization processes in volcanic suites. Contrib. Min. Pet., 60: 57-75.

Anderson, A.T., 1976. Magma Mixing: Petrological Process and Volcanological Tool. Jour. Volc. Geotherm. Res., 1: 3-33.

Arculus, R.J., and Wills, K.J.A., 1980. The petrology of plutonic blocks and inclusions from Lesser Antilles Island Arc. J. Petrol., 21, 743-799.

Arth, J.G., 1976. Behavior of trace elements during magmatic processes - a summary of theoretical models and their applications. Jour. Res. U.S.G.S., 4, 1: 41-47.

Ashwal, L.D., Leo, G.W., Robinson, P., Zartman., R.E., and Hall, D.J., 1979. The Belchertown Quartz Monzodiorite Pluton, West Central Massachusetts: A Syntectonic Acadian Intrusion. A. J. Sci., 279: 936-969.

Bailey, J.C., 1981. Geochemical Criteria for a Refined Tectonic Discrimination of Orogenic Andesites. Chem. Geol., 32, 139-154.

Bailey, E.B., and McAllien, W.J., 1950. The Ankara Melange and the Anatolian Thrust. M.T.A. Mecmuasi, 15, 40: 17-21.

Banner, J.L., 1981. Lolobau Island, New Britain: Petrology of an Island Arc Volcanic Complex. unpublished Master's thesis, State University of New York at Stonybrook.

Bence, A.E., and Albee, A.L., 1968. Empirical Correction Factors for the Electron Microanalysis of Silicates and Oxides. J. Geology, 76: 382-403.

Boyd, F.R., 1973. A Pyroxene Geotherm, Geochem. Cosmochem. Acta, 37, 12, 2533-2546.

Brinkmann, R., 1976. The Geology of Turkey. Elsevier Publ. Inc., Amsterdam, 158 pp.

Büsch, W., Schneider, G., and Mehnert, K.R., 1974. Initial Melting at Grain Boundaries, Part 2, Melting of Rocks of Granodioritic, Quartzdioritic, and Tonolitic Composition. Neues Jahrb. Mineral. Monatsh., 8: 345-370.

Büyükönal, Gönül, 1971. Microscopical study of the volcanic rocks around Ankara. Communications de la Faculté des Sciences de l'Université d'Ankara, v. 15c.

Cawthorn, R.G. and O'Hara, M.J., 1976. Amphibole Fractionation in Calc-Alkaline Magma Genesis. A.J. Sci., 276, 309-329.

Chaput, E., 1931. Notice explicative de la carte geologique à 1/135,000 de la région d'Angora (Ankara), Publ. de l'Institute de Géologie de l'Université de Stanboul, No. 7, Nov. 1931.

Cox, K.G., Bell, J.D., and Pankhurst, R.J., 1979. The Interpretation of Igneous Rocks. George Allen and Unwin Ltd., London, 450 pp.

Deer, W.A., Howie, R.A., and Zussman, J., 1963. Rock Forming Minerals; Vol. 2 Chain Silicates. Longmans, Green and Co., London, 379 pp.

Deer, W.A., Howie, R.A., and Zussman, J., 1978. Rock Forming Minerals; Vol. 2A Single Chain Silicates. Longman Group Ltd., London, 668 pp.

Deer, W.A., Howie, R.A., and Zussman, J., 1962. Rock Forming Minerals; Vol. 3 - Sheet Silicates. Longmans, Green and Co., London, 270 pp.

Dewey, J.F., Pitman, W.C., III, Ryan, W.B.F., and Bonnin, J., 1973. Plate tectonics and the evolution of the Alpine System, Geol. Soc. Am. Bull., 84: 3137-3180.

Dewey, J.F., and Şengör, A.M.C., 1979. Aegean and surrounding regions: complex multiplate and continuum tectonics in a convergent zone. Geol. Soc. Am. Bull., 90, pt. I: 84-92.

Dyer, J.M., 1982. Petrology of the Kula Volcanic Field, Western Turkey. unpubl. master's thesis, State University of New York at Albany.

Eggler, D.H. and Burnham, C.W., 1973. Crystallization and Fractionation Trends in the System Andesite - H_2O - CO_2 - O_2 at Pressures to 10 Kb. G.S.A. Bull., 84, 2513-2532.

Eichelberger, J.C., 1978. Andesitic volcanism and crustal evolution. Nature, 275: 21-27.

Eichelberger, J.C., 1975. Origin of Andesite and Dacite: Evidence of mixing at Glass Mountain in California and at other circum-Pacific volcanoes. G.S.A. Bull., 86, 1381-1391.

Erentoz, C., and Ketin, I., 1962. Explanatory Text of the Geological Map of Turkey, Sinop Sheet. Maden Tektik ve Arama Enstitusu Publ., Ankara.

Ernst, W.G., 1968. Amphiboles. Springer-Verlag Inc., New York, 125 pp.

Ewart, A., 1976. Mineralogy and Chemistry of Modern Orogenic Lavas - Some Statistics and Implications. Earth & Planet. Sci. Lett., 31, 417-432.

Fourcade, S., and Allegre, C.J., 1981. Trace Element Behavior in Granite Genesis: A Case Study - The Calc-Alkaline Plutonic Association from the Querigut Complex (Pyrenees, France). Contrib. Min. Pet., 76: 177-195.

Garcia, M.O., and Jacobson, S.S., 1979. Crystal Clots, Amphibole Fractionation and the Evolution of Calc-Alkaline Magmas. Contrib. Min. Pet., 69, 319-327.

Gill, J.B., 1978. Role of trace element partition coefficients in models of andesite genesis. Geochem. Cosmochem. Acta, 42: 709-724.

Green, T.H., and Ringwood, A.E., 1968. Genesis of the Calc-Alkaline Igneous Rock Suite. Contrib. Min. Pet. 18, 105-162.

Gust, D.A., 1981. Experimental, Petrologic, and Geochemical Studies on the Origins of Andesite. Ph.D. thesis, Australian National Univ.

Gust, D.A., and Johnson, R.W., 1981. Amphibole bearing inclusions from Boisa Island, Papua New Guines: Evaluation of the role of fractional crystallization in an andesitic volcano. Jour. Geology, in press.

Hanson, G.N., 1978. The Application of Trace Elements to the Petrogenesis of Igneous Rocks of Granitic Composition. Earth Planet. Sci. Lett., 38: 26.43.

Hedge, C.E., 1971. "Nickel in High-Alumina Basalts". Geoch. Cosmo. Act., v. 35, p. 522-524 (and reply by Taylor, et al., pp. 529-528.).

Helz, R.T., 1976. Phase Relations of Basalts in their Melting Ranges at PH_2O=5kb. Part II - Melt Compositions J. Petrol., 17, 139-193.

Hibbard, M.J., 1981. The Magma Mixing Origin of Mantled Feldspars. Contrib. Min. Pet., 76: 158-170.

Jakes, P., and Gill, J., 1970. Rare Earth Elements and the Island Arc Tholeiite Series. Earth Planet. Sci. Lett., v. 9, 17-28.

Jakes, P., and White, A.J.R., 1972. Major and Trace Element Abundances in Volcanic Rocks of Orogenic Areas. G.S.A. Bull., 83, 29-40.

Kay, R.W., 1980. Volcanic Arc Magmas: Implications of a melting-mixing model for element recycling in the crust-upper mantle system. Jour. Geology, in press.

Kerr, P.F., 1977. Optical Mineralogy. McGraw-Hill Book Co., New York, 492 pp., 4th edition.

Ketin, I., 1959. Türkiye'nin orojenik gelismesi. Maden Tektik Arama Dergisi, 53: 78-86.

Ketin, I., 1966. Tectonic units of Anatolia. Bull. Miner. Res. Expl. Inst. Turk., 66: 23-34.

Lofgren, G., 1974. An Experimental Study of Plagioclase Crystal Morphology: Isothermal Crystallization. Am. J. Sci., 274: 243-273.

McKenzie, D.P., 1972. Active Tectonics of the Mediterranean. Geophys. Jour. Royal Astron. Soc., 30: 109-185.

Minster, J.F., and Allegre, C.J., 1978. Systematic Use of Trace Elements in Igneous Processes, Part III. Inverse Problem of Batch Partial Melting in Volcanic Suites. Contrib. Min. Pet. 68, 37-52.

Miyashiro, A., and Shido, F., 1979. Tholeiitic and Calc-Alkaline Series in Relation to the Behaviors of Ti, V, Cr, and Ni. A. J. Sci., v. 275, p. 265-277.

Nicholls, I.A., and Whitford, D.J., 1976. Primary Magmas associated with Quaternary volcanism in the western Sunda arc, Indonesia. In: R.W. Johnson, ed., Volcanism in Australasia, Elsevier, Amsterdam, 77-90.

Pamir, H., and Erentoz, C., 1975. Explanatory Text of the Geological Map of Turkey, Ankara Sheet. Maden Tektik Arama Enstitusu Publ., Ankara.

Pearce, J.A., 1975. Basalt Geochemistry used to Investigate Past Tectonic Environments on Cyprus. Tectonophysics, v. 25, pp. 41-67.

Pearce, J.A., and Cann, J.R., 1971. Ophiolite Origin Investigated by Discriminant Analysis Using Ti, Zr, and Y. Earth Planet. Sci. Lett., v. 12, pp. 339-349.

Pearce, J.A., and Gale, G.H., 1977. Identification of Ore-Deposition Environment from Trace Element Geochemistry of Associated Igneous Host Rocks. In: Volcanic Processes in Ore Genesis, 1977, Spec. Publ. No. 7, Geol. Soc. London.

Pearce, J.A., and Norry, M.J., 1979. Petrogenetic Implications of Ti, Zr, Y, and Nb Variations in Volcanic Rocks. Contrib. Min. Pet., 69, 33-47.

Peccerillo, A., and Taylor, S.R., 1976. Geochemistry of Eocene Calc-Alkaline Volcanic Rocks from the Kastamonn Area, Northern Turkey. Contrib. Min. Pet., 58: 63-81.

Perfit, M.R., Gust, D.A., Bence, A.F., Arculus, R.J., Taylor, S.R., 1980. Chemical characteristics of island arc basalts: implications for mantle sources. Chem. Geol., v. 30, 227-256.

Phillips, W.R., 1971. Mineral Optics. W.H. Freeman and Co., San Francisco, 249 pp.

Phillips, W.R., and Griffen, D.T., 1981. Optical Mineralogy: the Non-opaque Minerals. W.H. Freeman and Co., San Francisco, 677 pp.

Ringwood, A.E., 1977. Petrogenesis in Island Arc Systems. In: Island Arcs, Deep Sea Trenches, and Back Arc Basins, M. Talwani and W.C. Pitman, III, eds., Maurice Ewing Series 1, A.G.U., 1977.

Schroeder, B., Thompson, G., Sulanowska, M., and Ludden, J.N., 1980. Analysis of Geologic Materials Using an Automated X-Ray Fluorescence System. X-Ray Spectronometry, 9, 4: 198-205.

Şengör, A.M.C., 1979. Mid-Mesozoic closure of Permo-Triassic Tethys and its implications. Nature, 279: 590-593.

Şengör, A.M.C., and Dyer, J.M., 1979. Neotectonic provinces of the Tethyan orogenic belt of the eastern Mediterranean: variations in tectonic style and magmatism in a collision zone (abs.). EOS, 60, 18: 390.

Şengör, A.M.C., and Kidd, W.S.F., 1979. Post-collisional tectonics of the Turkish-Iranian plateau and a comparison with Tibet. Tectonophysics, 55: 361-376.

Şengör, A.M.C., and Yilmaz, Y., 1981. Tethyan Evolution of Turkey: A Plate Tectonic Approach. Tectonophysics, 75: 181-241.

Şengör, A.M.C., Yilmaz, Y., and Ketin, I., 1980. Remnants of a pre-late Jurassic ocean in northern Turkey: fragments of Permian-Triassic Paleo-Tethys. Geol. Soc. Am. Bull., 91 (Part I): 499-609.

Taylor, S.R., Capp, and Graham, 1969, "Trace Element Abundancies in Andesites, II" Saipan, Bougainville, and Fiji. Contrib. Min. Pet., 23, 1: 1-26.

Taylor, S.R., Kay, M., White, A.J.R., Duncan, A.R., and Ewart, A., 1969. "Genetic Significance of Co, Cr, Ni, Sc, and V Content of Andesites". Geoch. Cosmo Acta., v. 33, 279-286.

Taylor, S.R., and White, A.J.R., 1965. Geochemistry of Andesites and the Growth of Continents. Nature 208, 271-273.

Walker, G.P.L., 1972. Crystal Concentration in Ignimbrites. Contrib. Min. Pet., 36: 135-146.

Watson, E.B., 1979. Zircon Saturation in Felsic Liquids: Experimental Results and Application to Trace Element Geochemistry. Contrib. Min. Pet., 70: 407-419.

White, A.J.R., and Chappell, B.W., 1977. Ultrametamorphism and Granitoid Genesis. Tectonophysics 43: 7-22.

Whitford, D.J., Nicholls, I.A., and Taylor, S.R., 1979. Spatial Variations in the Geochemistry of Quaternary Lavas Across the Sunda Arc in Java and Bali. Contrib. Min. Pet. 70, 341-356.

Williams, H., Turner, F.J., Gilbert, C.M., 1954. Petrography. W.H. Freeman and Co., San Francisco, 406 pp.

APPENDIX I - POTASSIUM-ARGON AGE DETERMINATION

Potassium-Argon Age Determination

A potassium-argon age determination was done on sample 9-10 by the Geochron Laboratories, Division of Krueger Enterprises, Inc. A biotite separate (about 90% biotite) was prepared by Geochron, and the age determination was performed on this separate. The results are listed below:

AGE = 42.0 $\pm$ 1.6 M.Y.

Ar^{40*}/K^{40} = .002487

Argon Analyses:

Ar^{40*},ppm.	Ar^{40}/Total Ar^{40}	Ave.Ar^{40*},ppm.
.01848	.800	.02022
.02196	.600	

Potassium Analyses:

% K	Ave. % K	K^{40},ppm.
6.646	6.665	8.131
6.685		

Constants Used:

$\lambda\beta = 4.72 \times 10^{-10}$/year

$\lambda_e = 0.585 \times 10^{-10}$/year

$K^{40}/K = 1.22 \times 10^{-4}$ g./g.

$$AGE = \frac{1}{\lambda_e + \lambda_\beta} \ln \frac{\lambda_\beta + \lambda_e}{\lambda_e} \times \frac{Ar^{40*}}{K^{40}} + 1$$

Note: Ar^{40*} refers to radiogenic Ar^{40}.
M.Y. refers to millions of years.

APPENDIX II - THIN SECTION DESCRIPTIONS

HIGH K BASALTIC ANDESITE

SAMPLE NO. 2-4

Texture

Porphyritic and intersertial. Some flow foliation is present in the groundmass.

Phenocryst Phases

Plagioclase - medium (mostly) to large (to 4mm) grains, some continuously zoned, most with oscillatory zoning. Grains shapes are generally somewhat rounded. Grains sometimes occur in pairs or small clots. Some highly altered grains (pseudomorphs) are present; one grain was observed where only the core was altered. Some antiperthite textures were seen in a few of the larger grains; these are xenocrysts perhaps.

Olivine - small to medium grains (to 1mm), frequently euhedral and showing six-sided sections. The grains are always altered around the rims to iddingsite with the smaller grains completely altered. Exsolution lamellae (?) were observed in one grain (as numerous fine lines) and slight zoning was evident in several grains. Composition was estimated optically to the around Fo_{75}.

Quartz - several large grains (~3mm) and a few smaller ones present. All are well corroded and are surrounded by reaction rims of very small, colorless grains of clinopyroxene and a brown alteration product.

Hornblende - small, irregularly shaped, relict grains which have been replaced by pyroxene.

Fe/Ti Oxides - numerous small (to 0.1mm), irregular grains are scattered about.

Groundmass

Plagioclase is the dominant groundmass (80-90%) and occurs as fairly large intergrown laths. A small amount of glass fills the interstices between the plagioclase laths. A few small, euheral grains of clinopyroxene are present. The smaller olivine grains could be considered part of the groundmass.

Estimated Mode (phenocrysts)

10% plagioclase
5% olivine
2% quartz
1% Fe/Ti oxides

18% Total

ANDESITE

SAMPLE NO. 11-9

Texture

Porphyritic and hyalopilitic with a strong flow foliation.

Phenocryst Phases

Plagioclase - small to large (to 6mm), euhedral to rounded phenocrysts. Slight continuous zoning in some grains with oscillatory and sometimes patchy zoning in others. About half the grains show a slight amount of alteration around the rims or in the cores.

Orthopyroxene - small to medium (to 0.5mm) euhedral grains. They are frequently zoned with pink pleochroic cores and colorless rims. The grains usually occur singly.

Clinopyroxene - euhedral grains of similar size to orthopyroxene. The phenocrysts are commonly twinned and frequently occur in clusters or clots.

Biotite - small to medium (to 1mm) grains. Shape varies from somewhat rounded grains without reaction rims to strongly corroded grains with rims of hornblende and opaques.

Hornblende - golden brown, medium sized (to 2mm), euhedral grains, with some cross sections exhibiting zoning.

Quartz - small to medium (to 1mm), rounded and embayed grains.

Fe/Ti Oxides - abundant, small (to 0.1 or 0.2mm), euhedral to subhedral grains.

Apatite - occurs as inclusions in hornblende and biotite.

Groundmass

Glass comprises 30 to 50% of the mesostasis with plagioclase microlites and continuously zoned microphenocrysts making up most of the rest. Fe/Ti oxides are very abundant, occurring as isometric euhedral to subhedral grains. Some microphenocrysts of euhedral clinopyroxene are present, as are small, golden brown, hexagonal plates of biotite.

Other Observations

Two clots are present in this thin section. The first is glomeroporphyritic and composed primarily of euhedral orthopyroxene grains, sometimes with clinopyroxene rims. The other phases present are small, continuously zoned plagioclase, Fe/Ti oxides, and brown glass.

The second clot is composed of brown hornblende, biotite, and plagioclase intergrown in a cumulate texture. Brown glass (partially deritrified) containing a few microlites fills some interstices and Fe/Ti oxides are scattered throughout.

Occasional small, round clusters of tiny clinopyroxene needles are present. The appearance of the needles, which radiate towards the center from the edges, suggests that they have grown in from the outside edge. The centers contain a small amount of glass.

Estimated Mode (phenocrysts)

15% plagioclase
5% hornblende
5% biotite
2% orthopyroxene
3% clinopyroxene
1% quartz
1% Fe/Ti oxides
32% Total

ANDESITE

SAMPLE NO. 7-4

Texture

Porphyritic and hyalopilitic.

Phenocryst Phases

Orthopyroxene - medium (to 2mm) non-pleochroic, euhedral grains, some twinned. Bronzite exsolution structures are sometimes present, and a few grains appear zoned. Some grains have thin quench rims. A brown alteration product is frequently present around the margins of the grains.

Clinopyroxene - small to medium, euhedral grains which occur singly or in small clots. Some grains are twinned, others are zoned.

Plagioclase - a few medium to large (to 4mm) rounded grains. Most shown continuous zoning with some mild oscillatory zoning. Alteration is frequent around the margins of grains.

Biotite - pseudomorphs composed of finely divided opaque granules.

Fe/Ti Oxides - many very small (< 0.1mm) grains with square cross sections scattered about.

Quartz - one rounded, embayed grain with a reaction rim of minutely crystalline clinopyroxene.

Groundmass

The groundmass is composed principally of small plagioclase laths with the interstices filled with glass that is devitrified in places. Small euhedral grains of orthopyroxene are also present, as is some secondary hematite.

Estimated Mode (phenocrysts)

5% orthopyroxene

10% clinopyroxene

4% plagioclase

1% biotite

1% Fe/Ti Oxides

21% Total

ANDESITE

SAMPLE NO. 21-5

Texture

Porphyritic and vitrophyric with some flow foliation in the glass. Phenocryst minerals are present as small, broken fragments in some areas of the slide.

Phenocryst Phases

Plagioclase - medium to large grains (to 5mm). Most are euhedral but some are slightly rounded and others are broken. Zoning is commonly oscillatory, but continuous or discontinuous zoning is sometimes present. Zones of dendritic growth are common. Large grains are composed of several carlsbad twins.

Hornblende - small to large (to 8mm) euhedral grains. The phenocrysts are bright olive green in lengthwise sections and strongly pleochroic from light brown to dark greenish brown in cross section. Numerous inclusions are present, including oxides, plagioclase, apatite, and orthopyroxene.

Orthopyroxene - small to medium grains (to 1mm), varying in shape from euhedral to subhedral. Strong pleochroism is evident.

Biotite - medium grains (to 2mm). It is usually associated with hornblende, oxides, and plagioclase in clots, where it is very irregularly shaped. Rounded shapes are exhibited when it occurs alone. Inclusions of plagioclase and apatite are common.

Fe/Ti Oxides - numerous, small (0.1 to 0.2mm), euhedral to anhedral grains are present.

Zircon - one grain occurring as a phenocryst was observed.

Groundmass

Glass containing crystallites composes 80-90% of the groundmass. The microphenocryst population consists of euhedral hornblende, euhedral orthopyroxene, and oxides.

Other Observations

One very large xenolith is present. It is composed of densely intergrown plagioclase laths and hornblende, with some small amount of orthopyroxene in a reaction relationship(?) with the hornblende. The grcundmass is composed of a small amount of colorless to brown glass that contains a few plagioclase microlites.

Estimated Mode - (phenocrysts)

55% plagioclase
15% hornblende
2% orthopyroxene
2% Fe/Ti oxides
1% biotite

75% Total

ANDESITE

SAMPLE NO. 8-4

Texture

Porphyritic, trachytic, and vesicular.

Phenocryst Phases

Clinopyroxene - small to medium (to 2mm, most smaller), euhedral grains. Slightly developed exsolution lamellae are sometimes present. Some grains are slightly zoned and twinning is frequent. The grains occur singly or in small clots.

Orthopyroxene - small, euhedral grains occurring singly or in small clots. The grains are commonly zoned with pleochroic cores and non-pleochroic rims.

Plagioclase - up to 4mm. Most grains are rounded, but some have euhedral shapes. Continuous zoning is the most common type, although oscillatory zoning is present in some grains.

Quartz - small (to 1mm), rounded grains with microcrystalline rims of clinopyroxene.

Biotite - a few medium grains (to 1mm), either rounded and corroded or completely altered to pseudomorphs composed of finely divided oxides.

Hornblende - occurs primarily as a few opaque pseudomorphs. One strongly corroded grain altered to oxides around the rim is present. Two of the pseudomorphs have rims of granular pyroxene.

Fe/Ti Oxides - small subhedral grains.

Groundmass

The primary groundmass is plagioclase, which occurs as very small

elongate to blocky microphenocrysts and as abundant microlites. The microphenocrysts are commonly strongly continuously zoned. Abundant tiny grains of Fe/Ti oxides are present, as are some euhedral microphenocrysts of clinopyroxene. Glass fill the interstices between the other phases and forms about 1/4 of the groundmass.

Other Observations

One round clump, about 2mm across, of inwardly radiating clinopyroxene is present.

Estimated Mode (phenocrysts)

10%	orthopyroxene
5%	clinopyroxene
5%	plagioclase
1%	Fe/Ti oxides
< 1%	each of quartz, biotite, and hornblende
24%	Total

ANDESITE

SAMPLE NO. 22-10

Texture

Porphyritic and hyalopilitic, with a slight flow foliation in the groundmass.

Phenocryst Phases

Plagioclase - small to large (to 4mm) grains. Shapes vary from slightly rounded, euhedral to very rounded, with a few grains appearing embayed. The grains occur singly or in small clusters. All types of zoning can be found, and zones of dendritic growth are well developed in the larger grains.

Orthopyroxene - small to medium (to 1.5mm), euhedral grains with alteration rims which occur singly or in small clumps, sometimes with a small amount of clinopyroxene. It also is found replacing hornblende.

Clinopyroxene - abundant, small (to 1mm), euhedral to subhedral, elongated grains.

Hornblende - medium to large (to 3mm), euhedral to rounded grains, all of which have been altered in either of two ways; to orthopyroxene or to dusty opaques.

Biotite - medium sized grains (to 1.5mm), in either irregularly corroded shapes or rounded shapes with some embayments. The corroded grains are surrounded by rims of plagioclase and oxides, while the larger roumded grains are partially altered to dusty opaques.

Quartz - a few small to medium (to 1mm), very rounded and embayed grains.

Fe/Ti oxides - abundant small to medium (to 0.2mm), subhedral to anhedral grains.

Groundmass

The groundmass consists primarily of a dense mat of plagioclase microphenocrysts and microlites in a glass (60%) matrix. Microphenocrysts of orthopyroxene are common, and very small grains of oxides are extremely numerous.

Estimated Mode (phenocrysts)

20%	plagioclase
5%	orthopyroxene
3%	clinopyroxene
3%	hornblende
2%	biotite
2%	quartz
1%	opaques
36%	Total

DACITE

SAMPLE NO. 22-6

Texture

Porphyritic and hyalopilitic to vitrophyric.

Phenocryst Phases

Plagioclase - small to large (to 6mm) grains, with the larger trending to be composed of several twins and intergrown grains. Oscillatory zoning is the most common type in the larger grains, with some patchy zoning also present. The smaller grains are usually continuously or discontinuously zoned. Some zones of dendritic growth are present. Inclusions of fluid, crystallites, and occasionally hornblende or zircon are found in the larger grains.

Hornblende - green, medium to very large (to 7mm) grains. Shapes range from euhedral with slight rounding, to very rounded and embayed irregular shapes. Some hornblende is rimmed by small orthopyroxene grains. Inclusions are frequent and include plagioclase, apatite, and zircon.

Orthopyroxene - small to medium (to 0.8mm), euhedral to subhedral grains that exhibit marked pleochroism. Phenocrysts occur singly, although small grains are found surrounding hornblende in a reaction relationship.

Biotite - a few small, very rounded and embayed grains are found, sometimes surrounded by oxides and fine-grained plagioclase in a reaction relationship. A few inclusions of apatite and oxides are present.

Quartz - a few small (to 0.8mm) very rounded grains.

Fe/Ti Oxides - small to medium (to 0.2mm) subhedral to large (to 0.8mm), very irregular anhedral grains.

Groundmass

Glass comprises about 90% of the groundmass. Plagioclase microphenocrysts (strongly zoned) and microlites are extremely abundant. Some microphenocrysts of orthopyroxene are also found.

Estimated Mode (phenocrysts)

45% plagioclase
10% hornblende
2% orthopyroxene
1% biotite
1% quartz
2% Fe/Ti Oxides

61% Total

DACITE

SAMPLE NO. 2-1

Texture

Porphyritic and pilotaxitic, with no apparent flow foliation.

Phenocryst Phases

Plagioclase - large (to 5mm) grains occurring singly or in clumps. Strong oscillatory zoning is present in most, although a few just exhibit continuous zoning. Inclusions of fluid and crystallites are common.

Hornblende - large, euhedral grains (to 4mm). All grains have been altered to oxides and hematite (?), although an unaltered core can sometimes be found. Most contain fluid inclusions.

Pyroxene - a number of small, highly altered grains are present whose shape suggests pyroxene. These grains exhibit golden brown rims with colorless, non-birefringent centers.

Biotite - medium, rounded and embayed, relict grains composed of granular oxides.

Quartz - a very few, small, embayed grains are present.

Fe/Ti Oxides - numerous, small (to 0.2mm), subhedral to anhedral grains.

Groundmass

The groundmass is a mixture of devitrified glass (about 3/4), plagioclase microlites, and small bits of brown altered material. A few small areas of non-devitrified glass can be found.

Estimated Mode (phenocrysts)

35% plagioclase

10% hornblende

2% pyroxene

2% biotite

1% Fe/Ti oxides

< 1% quartz

51% Total

DACITE

SAMPLE NO. 15-9

Texture

Porphyritic and hyalopilitic, with no flow foliation evident.

Phenocryst phases

Plagioclase - medium to large (to 4mm), euhedral to rounded grains, with some broken fragments. One grain has a very resorbed margin. Zoning ranges from patchy and oscillatory to discontinuous and continuous, with some zones of dendritic growth. Multiple twins are common. Fluid inclusions are common and one inclusion of hornblende was noted.

Hornblende - medium to large (to 2mm), euhedral grains. Many are unaltered, but some have rims of orthopyroxene and oxides, while others are completely altered to pseudomorphs composed of dusty oxides. A few grains show partially resorbed margins. This mineral usually occurs, alone, but is sometimes found in small clots with plagioclase, biotite, and oxides, in various combinations. Apatite and oxide inclusions are fairly common.

Biotite - medium (to 1mm), fairly euhedral to rounded to very corroded grains with fine-grained plagioclase and oxide rims. Some grains have apatite and/or oxide inclusions; one has inclusions of hornblende.

Quartz - small to medium grains (to 1.5mm), usually of rounded shape. One grain exhibits a euhedral shape with only slight embayments. Another is very rounded and surrounded by a reaction rim of tiny clinopyroxene.

Fe/Ti Oxides - medium (to 0.2mm), euhedral squares and hexes to anhedral grains.

Zircon - fairly large for zircon (0.1mm), fairly abundant anhedral grains.

Groundmass

Partially devitrified glass makes up about 3/4 of the groundmass. Plagioclase is again the dominant mineral phase, occurring both as continuously zoned microphenocrysts and as microlites. Orthopyroxene and clinopyroxene are found as euhedral microphenocrysts, as is hornblende. Tiny oxide grains are also common.

Estimated Mode (phenocrysts)

30% plagioclase
12% hornblende
5% biotite
2% quartz
1% Fe/Ti Oxides

50% Total

DACITE

SAMPLE NO. 22-2

Texture

Porphyritic and pilotaxitic, with a slight flow foliation.

Phenocryst Phases

Plagioclase - small to very large (to 8mm long), grains, usually euhedral, but sometimes slightly rounded. Oscillatory zoning is the most common type, although continuous or discontinuous zoning are present in some grains. A few zones of dendritic growth are present. Some grains are slightly altered.

Hornblende - small, anhedral fragments to large (4mm long), euhedral grains that occur singly or in clots with small amounts of plagioclase and oxides. Some grains have slightly embayed margins. Inclusions of plagioclase, apatite, and oxides are common; those of zircon are infrequent.

Biotite - medium (to 1mm), rounded to embayed grains, frequently with inclusions of plagioclase and apatite. Some grains have slight reaction rims of plagioclase and oxides.

Quartz - small to medium (to 0.8mm), rounded, embayed grains.

Fe/Ti Oxides - small to medium (to 0.2mm), euhedral to anhedral grains.

Groundmass

The groundmass is a cryptocrystalline mass of feldspar (?) and quartz (?) with a few zoned plagioclase microphenocrysts.

Estimated Mode (phenocrysts)

30% plagioclase

10% hornblende

5% biotite

3% quartz

2% Fe/Ti oxides

50% Total

DACITE

SAMPLE NO. 11-6B

Texture

Porphyritic and trachytic.

Phenocryst Phases

Plagioclase - medium to very large (to 7mm), euhedral grains, occurring singly or in small clots. Most show strong oscillatory zoning with or without patchy zoning or zones of dendritic growth.

Clinopyroxene - medium (to 0.8mm) euhedral grains, found singly or in small clots. Some have thin quench rims.

Orthopyroxene - medium, euhedral grains, usually occurring singly. One elongated grains has an overgrowth of clinopyroxene.

Biotite - medium (to 1mm) grains, partially to completely altered to finely divided oxides. Other grains have unaltered cores with rims of small plagioclase and oxides.

Hornblende - a few relict grains composed of fine oxides.

Quartz - a few small, rounded grains.

Fe/Ti Oxides - small to medium (to 0.2mm), euhedral to anhedral grains.

Groundmass

The mesostasis is composed of a very dense mat of plagioclase microphenocrysts and microlites with a small quantity (~ 1/3) of glass.

Estimated Mode (phenocrysts)

20%	plagioclase
5%	biotite
5%	hornblende
3%	orthopyroxene
2%	clinopyroxene
< 1%	quartz
1%	Fe/Ti oxides
37%	Total

DACITE

SAMPLE NO. 7-2

Texture

Porphyritic and trachytic, with exceptional flow foliation.

Phenocryst Phases

Plagioclase - large to very large (to 8mm), grains with either continuous or oscillatory zoning. Some zones of dendritic growth are present. Grains occur singly, as multiple carlsbad twins, or in small clumps. Most are euhedral, although some have slightly rounded margins. One clot of plagioclase with orthopyroxene and oxides is present.

Hornblende - pseudomorphs composed of fine oxide granules in characteristic euhedral hornblende shapes. One grain present has an unaltered core surrounded by oxide and small orthopyroxene grains. Grains are up to 4mm long.

Orthopyroxene - small to medium, euhedral grains (to 0.8mm), found singly or in clumps. Slight pleochroism is evident and the grains are frequently twinned.

Biotite - small to medium (to 1mm), square to rectangular pseudomorphs composed primarily of fine-grained oxides. A small amount of unaltered biotite is sometimes present in the cores.

Quartz - a few small to medium, rounded and embayed grains.

Clinopyroxene - small, euhedral grains occurring singly or in clumps with clinopyroxene.

Fe/Ti Oxides - small, subhedral to anhedral grains.

Groundmass

A dense, well foliated mass of plagioclase microlites and microphenocrysts comprises most of the groundmass. Numerous tiny oxide grains are scattered about and some glass is present (~ 1/4).

Estimated Mode (phenocrysts)

10%	plagioclase
3%	hornblende
3%	biotite
1%	orthopyroxene
1%	clinopyroxene
< 1%	quartz
1%	Fe/Ti Oxides
20%	Total

DACITE

SAMPLE NO. 15-8

Texture

Porphyritic and hyalopilitic with no obvious flow foliation.

Phenocryst Phases

Plagioclase - medium to very large (to 7mm) grains. Shapes are variable, including euhedral, rounded, slightly embayed, and broken fragments. All types of zoning are present, as are zones of dendritic growth. The grains occur singly or in intergrown clumps.

Hornblende - medium (to 2mm), euhedral to slightly embayed grains. Slight to complete alteration to dusty opaques affects the grains. Hornblende occurs singly, in monominerallic clots, or in clots with plagioclase + oxides $\pm$ biotite.

Biotite - small to medium (to 1.5mm) grains, usually very embayed and corroded and surrounded by a dense cloud of oxides granules and fine grained plagioclase.

Quartz - a very few small to medium (to 1mm) rounded and embayed grains.

Fe/Ti Oxides - very abundant, small to medium (to 0.2mm), euhedral squares to anhedral grains.

Zircon - one subhedral grain observed.

Groundmass

The groundmass consists of about 3/4 brown, partially devitrified glass containing abundant plagioclase microlites and continuously zoned microphenocrysts. Rod-shaped crystallites are also abundant.

Other Observations

One xenocryst composed of densely intergrown plagioclase laths and hornblende in a subophitic texture is present.

Estimated Mode (phenocrysts)

30% plagioclase
5% hornblende
2% biotite
1% quartz
2% Fe/Ti Oxides

40% Total

DACITE

SAMPLE NO. 14-1B

Texture

Porphyritic and hyalopilitic with no flow foliation.

Phenocryst Phases

Plagioclase - small to large (to 5mm) euhedral grains with a few broken ones present. All types of zoning can be observed. Some grains have thin zones of poorly developed dendritic growth.

Hornblende - medium to large (to 3mm) euhedral to rounded and embayed relict grains, composed of dusty oxides. A few inclusions of plagioclase and apatite are present. One very rounded, dark yellow-brown unaltered grain was found.

Biotite - small to medium (to 1.5mm), very corroded remnants surrounded by rims of fine-grained plagioclase and oxides; other grains are finely divided oxide pseudomorphs.

Clinopyroxene - small (to 0.5mm) euhedral grains occurring singly or in small clots.

Fe/Ti Oxides - small to medium (to 0.2mm), subhedral to anhedral grains.

Zircon - a very few anhedral grains present.

Groundmass

Plagioclase microphenocrysts and microlites in a glass matrix (~ 60%) comprises most of the groundmass. Both orthopyroxene and clinopyroxene occur as euhedral microphenocrysts (0.1 to 0.2mm) along with very small oxide granules.

Estimated Mode (phenocrysts)

25% plagioclase

5% hornblende

2% biotite

2% quartz

1% Fe/Ti Oxides

35% Total

DACITE

SAMPLE NO. 11-6A

Texture

Porphyritic and hyalopilitic with a strong flow foliation in the groundmass.

Phenocryst Phases

Plagioclase - medium to large (to 5mm) grains, generally euhedral in shape, although broken grains are frequent; a few are slightly rounded or corroded. Nearly all show strong oscillatory zoning, often in conjunction with patchy zoning and zones of dendritic growth. Smaller phenocrysts are strongly continuously zoned. Grains occur singly or in clots.

Hornblende - medium to large (to 2mm), euhedral, relict grains composed of finely divided oxides.

Clinopyroxene - small (to 0.5mm) euhedral grains, frequently with hematite stains around the margins. The grains may occur singly, but are usually found in monominerallic clots. One clot observed contained both clinopyroxene and orthopyroxene.

Orthopyroxene - small, euhedral grains with hematite stains as above. Grains are non-pleochroic and are found alone or in small clusters of two or three grains.

Biotite - found as medium sized (to 1mm), opaque relicts, or as strongly corroded grains with rims of granular oxides.

Quartz - a few rounded grains are present.

Fe/Ti Oxides - small to medium (to 0.5mm), euhedral (square) to anhedral grains frequently with a thin coat of hematite around the margins.

Groundmass

Glass containing numerous plagioclase microlites and microphenocrysts forms the groundmass.

Other Observations

One xenolith is present. It is composed of a mat of fine-grained plagioclase and needle-like hornblende that has been altered to a reddish brown material (hematite ?). A few euhedral orthopyroxene grains can be found in this xenolith and a moderate flow foliation is present.

Patches of opal or tridymite occur as void fillings in places.

Estimated Mode (phenocrysts)

25%	plagioclase
5%	hornblende
2%	biotite
1%	orthopyroxene
1%	clinopyroxene
< 1%	quartz
1%	Fe/Ti Oxides
36%	Total

DACITE

SAMPLE NO. 14-1A

Texture

Porphyritic and hyalopilitic with a moderate flow foliation.

Phenocryst Phases

Plagioclase - medium to large (to 4mm), euhedral grains, with a few rounded grains and a few broken grains also present. Oscillatory and patchy zoning are common, as are zones of dendritic growth, although some grains simply have continuous or discontinuous zoning. Many grains contain inclusions of fluid and crystallites.

Hornblende - Medium to large (to 3mm), euhedral, relict grains, now composed of finely divided opaques. A few grains still have a small amount of unaltered golden brown hornblende in their cores.

Biotite - small (to 0.5mm) grains, which are corroded and rimmed by oxide granules.

Quartz - small to medium, rounded and embayed grains.

Apatite - one euhedral grain was observed.

Fe/Ti Oxides - abundant small (to 0.2mm), subhedral to rounded grains, with a few larger (to 0.8mm) irregular grains.

Groundmass

The groundmass consists of about 80% partially devitrified glass. Very abundant plagioclase microlites and microphenocrysts make up most of the remainder. Small oxide grains are numerous.

Estimated Mode (phenocrysts)

15% plagioclase

5% hornblende

2% biotite

1% quartz

2% Fe/Ti Oxides

30% Total

DACITE

SAMPLE NO. 21-2

Texture

Porphyritic and vitrophyric, with a strong flow foliation in the groundmass. The texture is fairly suggestive of compressed glass shards (eutaxitic texture).

Phenocryst Phases

Plagioclase - small to large (to 4mm), euhedral to somewhat rounded grains. Many small, broken fragments are present. Oscillatory zoning is the most common type, with continuous or discontinuous zoning present in some grains. Zoning appears to be reverse at the margins of some grains. Zones of well developed dendritic growth are common. Inclusions of crystallites and fluid are frequently present; one inclusion of zircon was observed.

Hornblende - medium to large (to 3mm), euhdral grains. They are frequently slightly embayed or corroded around the margins and occasionally are very corroded. Small inclusions of plagioclase, oxides, and apatite are frequent. Grains occur singly or with plagioclase in clots.

Biotite - medium to large (to 4mm), irregularly shaped grains intergrown with plagioclase, hornblende, and oxides. Frequently with apatite inclusions; one contains a large euhedral zircon inclusion.

Orthopyroxene - small to medium (to 0.5mm), subhedral to euhedral grains showing good pleochroism. Occasional larger grains (to 1mm) are present.

Fe/Ti Oxides - small (to 0.1mm), euhedral to anhedral grains.

Groundmass

The groundmass is composed predominantly of glass (about 80%) containing a few crystallites. The microphenocryst population includes plagioclase, hornblende, and oxides.

Other Observations

Two types of clots are present in this sample. The first is composed of plagioclase and hornblende in a glomeroporphyritic texture. The second is composed of a subophitic intergrowth of plagioclase laths and orthopyroxene with minor amounts of oxides present.

Estimated Mode (phenocrysts)

20% plagioclase
5% hornblende
3% biotite
1% orthopyroxene
1% Fe/Ti Oxides

30% Total

DACITE

SAMPLE NO. 1-2

Texture

Porphyritic and vitrophyric with a slight flow foliation.

Phenocryst Phases

Plagioclase - medium to large (to 5mm), generally euhedral grains. A fair number of broken fragments are present. Zoning ranges from oscillatory and patchy to continuous or discontinuous. Some grains have rounded cores with euhedral overgrowths of a different An content.

Hornblende - occurs either as medium to large (to 3mm) euhedral grains, single or in clumps, or as smaller subhedral grains in clots with plagioclase $\pm$ biotite. Grains frequently show simple twinning and may contain inclusions of oxides, fluid, or apatite. Pleochroism is strong, from green to golden brown.

Biotite - occurs as irregularly shaped grains in intergrown clots with plagioclase, hornblende, and oxides, or occurs as corroded, single grains surrounded by a rim of fine-grained plagioclase and granular oxides.

Orthopyroxene - small to medium (to 0.5mm), euhedral grains showing strong pleochroism. One large (2mm), irregular grain is surrounded by a rim of intergrown small hornblende grains.

Fe/Ti Oxides - small to medium, subhedral to irregular grains scattered throughout.

Groundmass

The groundmass is about 80% glass containing numerous tiny rod-

shaped crystallites. Microphenocrysts of plagioclase, hornblende, and orthopyroxene are very common.

Estimated Mode (phenocrysts)

30% plagioclase
6% hornblende
2% biotite
1% orthopyroxene
1% Fe/Ti Oxides

40% Total

DACITE

SAMPLE NO. 15-3B

Texture

Porphyritic and hyalopilitic with no obvious flow foliation.

Phenocryst Phases

Plagioclase - medium to large (to 4mm), euhedral to slightly rounded and embayed grains, often broken. Grains are found singly or in intergrown clumps. Most show strong oscillatory $\pm$ patchy zoning, although some simply display continuous zoning.

Hornblende - large (to 6mm), euhedral, relict grains composed of finely divided oxides. One unaltered, tan, euhedral grain was observed.

Biotite - Medium grains (to 1mm), most of which are opaque relicts. Some grains consist of an unaltered biotite core surrounded by a rim of fine-grained plagioclase and oxides.

Quartz - a few, small, rounded and embayed grains are present.

Clinopyroxene - one grain, identified as titano (?) aegirine-augite was observed.

Orthopyroxene - one grain was found. It was non-pleochroic and was mantled by clinopyroxene or pigeonite.

Allanite - one medium (0.5mm), rounded grain present.

Fe/Ti Oxides - numerous, medium-sized, euhedral to subhedral squares and hexes.

Zircon - two tiny grains present.

Groundmass

The groundmass is composed of about 2/3 glass with various microphenocrysts making up the rest. Plagioclase is the most common mineral, occurring as both microphenocrysts and microlites. Small euhedral microphenocrysts of both orthopyroxene and clinopyroxene are common, with the clinopyroxene sometimes found in small clots. Tiny euhedral square grains of oxides are frequent, and crystallites are very abundant.

Other Observations

Rock fragments (xenoliths) of fine-grained, intergrown plagioclase and altered hornblende are present.

Estimated Mode

30% plagioclase
5% hornblende
2% biotite
1% quartz
2% Fe/Ti Oxides

40% Total

DACITE

SAMPLE NO. 9-8B

Texture

Devitrification has obscured the texture, but the many streaks and bands are suggestive of compressed glass shards(possible parataxitic or eutaxitic texture).

Phenocryst Phases

Plagioclase - large (to 4mm), euhedral grains, frequently broken. Zoning may be oscillatory or continuous. Inclusions of small biotite grains are sometimes found.

Biotite - small to medium (to 1mm) grains of irregular, corroded shape. The grains are surrounded by rims of fine-grained plagioclase and oxides.

Quartz - small to large (to 2mm) rounded grains, some of which are broken.

Fe/Ti Oxides - very small to small (to 0.1mm), euhedral squares and rectangles to rounded subhedral shapes.

Groundmass

The groundmass is composed mostly of glass (~ 60%) that contains numerous microlites and microphenocrysts of plagioclase and abundant crystallites.

Other Observations

Several rock fragments (xenoliths) composed of plagioclase microphenocrysts in an oxidized, tan groundmass are present.

Irregularly shaped blebs of devitrified to nondevitrified glass and of amorphous silica (?) are also present in this sample.

Estimated Mode (phenocrysts)

3% plagioclase

3% biotite

3% quartz

1% Fe/Ti Oxides

10% Total

DACITE

SAMPLE NO. 9-9

Texture

Porphyritic and hyalopilitic.

Phenocryst Phases

Plagioclase - very large (to 8mm), euhedral to rounded grains, sometimes broken. The grains occur singly or in clots. All types of zoning are present.

Biotite - rounded and sometimes corroded, small to medium grains (to 1mm). Inclusions of plagioclase, zircon, and apatite are present.

Quartz - very large (to 6mm), rounded and embayed grains. Some grains are broken and others appear to have very slight reaction rims.

Hornblende - a few small, relict oxide psuedomorphs are present. One slightly altered, euhedral grain was observed.

Fe/Ti Oxides - a few small (mostly) to large (to 0.8mm), subhedral grains are present.

Apatite - small grains which occur singly or as inclusions in biotite. Shapes are irregular to subhedral.

Groundmass

The groundmass is composed of about 70% glass that is partially devitrified. Plagioclase microlites and continuously zoned microphenocrysts are abundant, as are crystallites.

Other Observations

One large clot is present consisting of strongly continuously zoned plagioclase laths with the interstices filled with glass, biotite, and oxides.

Irregularly shaped blebs of a transparent, high relief material (amorphous silica ?) are present.

Estimated Mode (phenocrysts)

15%	plagioclase
8%	quartz
5%	biotite
< 1%	hornblende
1%	Fe/Ti oxides
30%	Total

DACITE

SAMPLE NO. 9-12A

Texture

Porphyritic and hyalopilitic, with the phenocrysts in a very haphazard and jumbled arrangement.

Phenocryst Phases

Plagioclase - small to large (to 5mm), euhedral to rounded grains that are usually broken into fragments of various sizes. All types of zoning can be observed.

Biotite - small to large (to 2mm) grains, generally euhedral, although frequently broken and sometimes slightly rounded. Some grains contain a few small apatite inclusions.

Quartz - small, rounded grains and broken grain fragments.

Fe/Ti Oxides - small to large (to 0.8mm), euhedral cubic to rounded grains. Some grains have anhedral shapes and very irregular (corroded ?) margins.

Zircon - two large (~ 0.2mm) grains are present. One is of euhedral shape and the other is an anhedral fragment.

Hornblende - infrequent, small (to 0.8mm), rounded, golden brown grains.

Groundmass

Tan, partially devitrified glass comprises most of the groundmass (~ 75%). Plagioclase microphenocrysts and microlites make up most of the rest, with a few biotite microphenocrysts also present.

Estimated Mode (phenocrysts)

20%	plagioclase
5%	biotite
3%	quartz
< 1%	hornblende
1%	Fe/Ti oxides
30%	Total

RHYOLITE

SAMPLE NO. 12-8

Texture

Porphyritic and hyalopilitic to pilotaxitic.

Phenocryst Phases

Plagioclase - medium to large (to 3mm), euhedral to somewhat rounded grains. Slight alteration sometimes affects the rims or cores of grains. Some grains show slight continuous zoning while others have well developed oscillatory zoning.

Biotite - medium sized grains (to 1.5mm). Shapes are either slightly rounded euhedral, or very corroded and surrounded by a rim of fine-grained plagioclase and oxides.

Quartz - medium to large (to 4mm), rounded and embayed grains.

Hornblende - medium (to 2mm), euhedral, relict grains composed of dusty oxides.

Pyroxene - several small (to 0.5mm), altered, relict, euhedral grains are present whose shapes suggest pyroxene.

Fe/Ti Oxides - small, subhedral grains.

Groundmass

The groundmass is composed of about 2/3 glass that is mostly devitrified. Plagioclase microlites and microphenocrysts are the principal mineral phase. The oxidized nature of this slide makes the groundmass composition difficult to determine.

Other Observations

Opal or tridymite is present in small amounts as void fillings.

Estimated Mode (phenocrysts)

25% plagioclase

3% biotite

2% hornblende

2% quartz

1% pyroxene (?)

1% Fe/Ti oxides

34% Total

RHYOLITE

SAMPLE NO. 9-10

Texture

Porphyritic and hyalopilitic with a strong flow foliation. Some streaks in the groundmass are suggestive of compressed glass shards (possible parataxitic texture).

Phenocryst Phases

Plagioclase - small to large (to 4mm), euhedral, rounded, or broken grains. Zoning ranges from slight continuous to strong oscillatory. Some thin zones of poorly developed dendritic growth are present. The smaller grains are broken fragments of larger crystals. One grain contains an inclusion of zircon.

Quartz - medium to large (to 5mm), rounded and embayed grains. Some grains are broken fragments.

Biotite - medium to large (to 2mm), euhedral grains, frequently somewhat rounded. Bent and broken grains are frequent. Plagioclase and apatite inclusions are frequently found.

Hornblende - small, euhedral grains (to 0.8mm), with one embayed grain present. Zoning is evident under crossed Nicols.

Fe/Ti Oxides - large (to 0.8mm), euhedral to rounded grains.

Orthopyroxene - one small, euhedral grain present.

Apatite - occasional small grains.

Groundmass

Slightly devitrified glass makes up about half the groundmass with blocky, continuously zoned microphenocrysts and slender microlites of plagioclase comprising the remainder.

Estimated Mode (phenocrysts)

15% quartz

10% plagioclase

3% biotite

2% hornblende

1% Fe/Ti oxides

31% Total

RHYOLITE

SAMPLE NO. 9-1

Texture

Porphyritic and pilotaxitic with a mild flow foliation.

Phenocryst Phases

Plagioclase - large (to 3mm), euhedral, rounded, or broken grains. Oscillatory, continuous, and discontinuous zoning can all be observed, along with a few thin zones of dendritic growth.

Quartz - numerous, large (to 3mm), rounded grains are present.

Biotite - medium to large (to 1mm), generally euhedral grains. Some are broken and others have irregular embayed margins. One grain contains small inclusions of plagioclase.

Hornblende - most grains are completely altered relicts composed of finely divided oxides and colorless material. A few grains contain unaltered hornblende in their cores. Maximum size is about 0.5mm.

Fe/Ti Oxides - mostly small to very small, euhedral grains with square, hexagonal, or octahedral shapes. A couple of very large (to 2mm), rounded grains and one clump of small, rounded grains are present.

Zircon - one large (~ 0.2mm), euhedral grain was observed.

Groundmass

The groundmass is primarily a dense mass of plagioclase microphenocrysts and microlites with a slightly devitrified glass matrix. Glass makes up about a third of the groundmass.

Estimated Mode (phenocrysts)

15% plagioclase

7% quartz

5% biotite

2% hornblende

1% Fe/Ti oxides

30% Total

APPENDIX III - MINERAL ANALYSES

Clinopyroxenes

	7-4B				11-9	8-4
SiO_2	52.71	52.12	54.79	52.71	53.86	52.99
Al_2O_3	3.28	3.87	2.40	3.06	2.39	2.21
TiO_2	0.48	0.56	0.36	0.45	0.42	0.39
FeO	5.41	5.97	6.06	5.53	5.69	5.56
MnO	0.19	0.19	0.19	0.17	0.22	0.20
MgO	16.75	17.06	22.38	17.50	16.29	16.01
CaO	20.38	21.36	14.49	20.74	21.32	20.05
Na_2O	0.40	0.39	0.21	0.38	0.42	0.35
K_2O	0.07	0.04	0.07	0.05	0.06	0.00
Cr_2O_3	0.27	0.33	0.28	0.42	0.59	0.28
						P 0.03
	99.94	101.89	101.23	101.01	101.26	98.07
En	48.48	47.55	61.64	49.13	46.63	43.49
Wo	42.42	42.81	28.69	41.89	43.87	45.40
Fs	9.10	9.64	9.66	8.98	9.50	11.11

Orthopyroxenes

	7-4B					11-9		8-4
SiO_2	56.15	56.53	56.22	55.21	56.06	55.78	55.88	53.86
Al_2O_3	1.93	1.23	1.61	2.69	3.29	1.43	1.33	2.08
TiO_2	0.14	0.10	0.13	0.23	0.06	0.12	0.10	0.24
FeO	9.03	9.06	7.68	11.72	7.08	7.55	7.61	9.85
MnO	0.25	0.22	0.17	0.29	0.20	0.24	0.18	0.25
MgO	31.46	31.15	31.82	28.61	31.61	31.56	31.79	29.23
CaO	1.56	1.76	1.65	1.58	1.66	1.78	1.43	1.70
Na_2O	0.07	0.05	0.03	0.04	0.04	0.08	0.08	0.00
K_2O	0.02	0.03	0.02	0.03	0.02	0.01	0.03	0.00
Cr_2O_3	0.32	0.14	0.52	0.18	0.72	0.61	0.61	0.18
								P 0.00
	100.93	100.27	99.85	100.58	100.74	99.16	99.04	97.40
En	83.24	82.80	85.05	78.41	85.68	84.82	85.48	77.14
Wo	2.97	3.35	3.16	3.11	3.24	3.43	2.76	3.74
Fs	13.78	13.84	11.79	18.48	11.08	11.75	11.76	19.12

Feldspar

2-1

	Lg Feld (C)	Lg Feld (R)	Feld (C)	Feld R	C Zoned Feld	½ way Zoned Feld	R Zoned Feld
SiO_2	58.62	59.89	60.49	55.34	59.15	59.48	60.09
Al_2O_3	25.72	25.55	24.82	27.73	25.86	25.22	24.90
TiO_2	0.03	0.01	0.00	0.04	0.04	0.02	0.03
FeO	0.25	0.25	0.23	0.46	0.23	0.25	0.26
MnO	0.02	0.02	0.00	0.02	0.04	0.00	0.02
MgO	0.00	0.03	0.00	0.02	0.01	0.00	0.00
CaO	8.54	8.30	7.44	11.15	8.57	7.88	7.35
Na_2O	6.30	6.66	6.95	5.00	6.60	6.88	7.05
K_2O	0.44	0.46	0.53	0.28	0.50	0.57	0.51
Cr_2O_3	0.00	0.00	0.00	0.01	0.00	0.00	0.00
P_2O_5	0.05	0.01	0.00	0.00	0.03	0.00	0.01
	99.98	101.10	100.45	100.04	101.03	100.30	100.22

Formulation

Si	2.625	2.648	2.686	2.500	2.627	2.653	2.679
Al	1.357	1.331	1.299	1.475	1.353	1.326	1.308
Ti	--	--	--	--	--	--	--
Fe	0.009	0.009	0.008	0.017	0.008	0.009	0.009
Mn	--	--	--	--	0.001	--	--
Mg	--	0.001	--	--	--	--	--
Ca	0.408	0.392	0.353	0.539	0.406	0.375	0.350
Na	0.546	0.571	0.597	0.437	0.568	0.594	0.609
K	0.025	0.024	0.028	0.016	0.027	0.031	0.028
Cr	--	--	--	--	--	--	--
P	0.001	--	--	--	--	--	--
	4.971	4.976	4.970	4.983	4.990	4.988	4.983

Feldspar (cont'd)

	22-6			8-4		
	Homo-geneous Feld(C)	Homo-geneous Feld(R)	Sm. Feld(C)	Sm. Feld(R)	Sm. Feld	G mass Feld
SiO_2	59.17	59.95	53.90	57.32	57.69	55.49
Al_2O_3	25.65	24.85	28.70	26.29	26.68	24.50
TiO_2	0.01	0.04	0.06	0.04	0.09	0.15
FeO	0.21	0.26	0.55	0.37	0.79	3.05
MnO	0.04	0.00	0.02	0.00	0.00	0.05
MgO	0.03	0.00	0.07	0.03	0.11	0.91
CaO	8.22	7.64	11.87	8.92	11.06	9.43
Na_2O	6.73	6.99	4.59	6.11	5.25	4.94
K_2O	0.44	0.56	0.25	0.39	0.32	0.70
Cr_2O_3	0.00	0.00	0.01	0.02	0.00	0.01
P_2O_5	0.00	0.00	0.01	0.01	0.05	0.16
	100.50	100.28	100.03	99.49	102.05	99.38
Formulation						
Si	2.635	2.673	2.441	2.586	2.553	2.549
Al	1.346	1.306	1.531	1.397	1.391	1.326
Ti	--	--	0.001	--	0.002	0.004
Fe	0.008	0.009	0.020	0.013	0.028	0.116
Mn	0.001	--	--	--	--	0.001
Mg	0.001	--	0.004	0.001	0.006	0.062
Ca	0.392	0.363	0.575	0.430	0.523	0.463
Na	0.582	0.604	0.402	0.533	0.449	0.439
K	0.024	0.031	0.013	0.022	0.017	0.070
Cr	--	--	--	--	--	--
P	--	--	--	--	0.001	0.005
	4.986	4.986	4.987	4.983	4.970	5.006

Feldspar (cont'd)

	1-2		7-2	
	Lg Feld(C)	Lg Feld(R)	Lg Feld(C)	Lg Feld(R)
SiO_2	59.36	60.73	60.02	59.48
Al_2O_3	25.06	24.44	24.77	25.12
TiO_2	0.04	0.03	0.03	0.05
FeO	0.20	0.27	0.23	0.29
MnO	0.02	0.01	0.00	0.00
MgO	0.02	0.02	0.01	0.00
CaO	7.81	7.21	7.51	7.61
Na_2O	6.84	7.14	6.86	6.81
K_2O	0.41	0.44	0.75	0.61
Cr_2O_3	0.00	0.01	0.00	0.00
P_2O_5	0.02	0.05	0.00	0.00
	99.79	100.34	100.17	99.99
Formulation				
Si	2.659	2.700	2.678	2.661
Al	1.324	1.281	1.303	1.325
Ti	0.001	0.001	0.001	0.002
Fe	0.007	0.010	0.009	0.011
Mn	0.001	--	--	--
Mg	0.001	0.001	0.001	0.000
Ca	0.375	0.344	0.359	0.365
Na	0.594	0.615	0.593	0.591
K	0.023	0.025	0.043	0.035
Cr	--	--	--	--
P	--	--	--	--
	4.986	4.978	4.987	4.988

Hornblende

	22-6		1-2
	Green	Green	Green
SiO_2	49.34	48.57	50.38
Al_2O_3	6.00	5.93	5.53
TiO_2	1.29	1.46	1.11
FeO	11.82	11.28	11.90
MnO	0.41	0.34	0.41
MgO	15.65	15.77	16.02
CaO	11.07	11.18	10.48
Na_2O	1.32	1.43	1.22
K_2O	0.35	0.32	0.21
Cr_2O_3	0.00	0.00	0.00
P_2O_5	0.04	0.05	0.01
	97.29	96.33	97.27

Formulation (on the basis of 23 oxygen)

Si	7.166	7.120	7.289
Al	1.023	1.024	0.942
Ti	0.136	0.159	0.119
Fe	1.437	1.381	1.439
Mn	0.047	0.039	0.046
Mg	3.389	3.446	3.455
Ca	1.722	1.755	1.622
Na	0.371	0.404	0.339
K	0.063	0.056	0.038
Cr	--	--	--
P	0.004	0.004	--
	15.358	15.387	15.289

Glass in Thin Section

	11-9	21-5(1)	21-5(2)		2-1
SiO_2	74.26	76.02	74.19		72.67
Al_2O_3	11.97	12.45	12.95		17.84
TiO_2	0.26	0.10	0.18		0.16
FeO	0.70	0.41	0.75		0.32
MnO	0.00	0.00	0.01		0.01
MgO	0.11	0.08	0.39		0.00
CaO	1.15	0.86	1.31		2.50
Na_2O	3.36	2.76	3.31		5.07
K_2O	3.56	4.92	4.32		4.01
Cr_2O_3	0.00	0.00	0.00		0.00
	95.37	97.60	97.41	P_2O_5	0.03
					102.60

CIPW Norms

a	38.07	38.90	34.51	32.98
c	0.50	1.02	0.45	5.34
or	21.04	29.08	25.53	25.53
ab	28.43	23.35	28.01	28.01
an	5.71	4.27	6.50	6.50
di	0.00	--	--	--
hy	1.13	0.79	2.07	2.10
cn	0.27	0.20	0.97	0.97
fs	0.86	0.59	1.10	1.13
ol	--	--	--	--
il	0.49	0.19	0.34	0.30
Total	95.37	97.60	97.41	100.76

APPENDIX IV - MAJOR ELEMENT MODELLING

Major Element Modelling

Major element modelling was done by hand on a programmable calculator, using the following mineral subtraction equation for each element:

$$C_{pm} - f\,(x\,C_{min\ 1} + yC_{min\ 2} + \ldots + zC_{min\ n}) = C_{rl}$$

where C_{pm} = concentration of an element in the parental magma

C_{min} = concentration of an element in a mineral phase

C_{rl} = concentration of an element in the residual liquid

f = fraction of solids removed

x, y, and z = fraction of mineral phase in extract

The concentrations of an element in the parental magma and in the minerals are known and the variables f, x, y, and z were systematically varied and adjusted until, for all elements, the calculated C_{rl} was in good agreement with the observed C_{rl}.